ON THE IDENTIFICATION OF THE FRICTION COEFFICIENT IN A SEMILINEAR SYSTEM FOR GAS TRANSPORT THROUGH A NETWORK*

MICHAEL HINTERMÜLLER[‡†] AND NIKOLAI STROGIES[‡]

Abstract. An identification problem for the friction parameter in a semilinear system of balance laws, describing the transport of gas through a passive network of pipelines, is considered. The existence of broad solutions to the state system is proven and sensitivity results for the corresponding solution operator are obtained. The existence of solutions to the output least squares formulation of the identification problem, based on noisy measurements over time at fixed spatial positions is established. Finally, numerical experiments validate the theoretical findings.

1. Introduction. The transport of natural gas through a single pipe can be modeled by a simplification of the full Euler equations, describing the conservation of mass as well as balance of momentum and energy in fluid dynamics. Assuming a heat flux through the pipe walls compensating discontinuities of temperature in case of shock- and rarefaction waves, energy is no longer a balanced quantity (see [16, Section 14.6]). Working under such a regime, an associated system approximately describing the underlying physics is given by

$$\begin{aligned} \rho_t + q_x &= 0, \\ q_t + (p(\rho) + \tfrac{q^2}{\rho})_x &= \lambda \tfrac{q|q|}{\rho} - g\rho h', \end{aligned} \tag{1}$$

which is a well known model for gas transport, see, e.g., [3, 8, 12]. Here, ρ, q, g, h' denote density, volume flow, gravitational constant and slope of the pipe, respectively. Further, $p(\rho)$ represents the pressure depending on the density of the natural gas, and λ is the friction coefficient, also known as Darcy friction factor, quantifying the influence of friction at the pipe wall on the flow behavior. Assuming additional simplifications in (1), like considering only planar networks with $h' \equiv 0$, neglecting the influence of $\frac{q^2}{\rho}$ in the flux term and utilizing the simplified pressure law $p(\rho) = a^2\rho$, where $a > 0$ denotes the constant speed of sound, we obtain a semilinear system of first-order partial differential equations. Defined on a pipe which is represented by the interval (x_L, x_R) with $x_L < x_R$, it is given by

$$\begin{aligned} \rho_t + q_x &= 0, \\ q_t + a^2\rho_x &= -\lambda \frac{q|q|}{\rho}, \end{aligned} \quad \text{on } (0,T) \times (x_L, x_R), \tag{2}$$

where $T > 0$ represents the time horizon. A brief discussion of the above mentioned simplifications can be found in [8, 21]. To obtain a well posed forward problem, we in addition consider the initial conditions

$$\rho(0,\cdot) = \rho_0(\cdot), \quad q(0,\cdot) = q_0(\cdot) \text{ for } x \in (x_L, x_R), \tag{IC}$$

and boundary conditions. System (2) is strictly hyperbolic with one strictly negative and one strictly positive eigenvalue. Consequently, conditions on linear combinations of the state variables ρ and q are required at both ends of the pipe. In other words, there have to exist certain vectors $c_L, c_R \in \mathbb{R}^2$ and functions $d_L, d_R \in L^\infty(0,T)$ such that

$$c_L^\top(\rho(t,x_L), q(t,x_L)) = d_L(t), \quad c_R^\top(\rho(t,x_R), q(t,x_R)) = d_R(t). \tag{BC}$$

In this work we are interested in identifying λ from time-continuous measurements of ρ at prespecified locations x. In this context, it is worth mentioning that identifying parameters in partial

* This work is supported by the German Research Foundation (DFG) within project B02 of CRC TRR 154

†Department of Mathematics, Humboldt-University of Berlin, Unter den Linden 6, 10099 Berlin, Germany (hint@math.hu-berlin.de)

‡Weierstrass Institute for Applied Analysis and Stochastics, Mohrenstraße 39, 10117 Berlin, Germany (hintermueller@wias-berlin.de, strogies@wias-berlin.de)

differential equations describing transport trough pipes naturally face a problem with respect to observability of data. In fact, associated optimal control problems involving one-dimensional conservation laws are usually formulated such that the objective is evaluated on subsets of the spatial domain with positive Lebesgue measure (see, e.g., [9, 13, 18, 23]) which is mostly due to the regularity of entropy solutions of conservation laws. In case of a pipeline, however, such data are most likely not available since usual measuring devices are installed at fixed positions and measure over time. Consequently, the identification problem has to be solved based on measurements taken at fixed positions in the spatial domain over time, only. A further consequence of this lack of observability is the limited knowledge on initial data since they can not be observed either.

Qualitatively, λ generates a pressure drop of the natural gas during the transportation through the pipeline, introducing the necessity of compressor stations when the species is transported over large distances. Knowledge on λ allows for a detailed quantification of the pressure drop that has to be compensated at each of these stations allowing for a more precise cost management by the operating company. In addition, the value of the friction coefficient plays an important role in simulating networks. In [21], besides other model parameters like pipe diameter or cross section, the influence of the friction coefficient on simulation procedures for gas transport has been investigated. In that work, the sensitivity of results to a single time step in several discretization schemes with respect to variations of λ was quantified with error control in mind. The quantification of the friction coefficient in terms of an inverse problem based on real measurement data is important since in practice it is only approximated, while the other parameters can be measured directly. Approximation formulas for λ like the Colebrook-White equation, Panhandle-A or -B and Chens equation are only valid in certain (p, q)-regimes and thus still introduce an error in to the simulation problem. A comprehensive discussion of approximating formulas for the friction coefficient along with the associated operating regimes can be found in [4]. Finally, traditionally the friction coefficient is assumed to be constant along the entire pipeline elements of a network. However, any single pipe in such a system may allow small variations of the friction coefficient due to production imperfections (in case of the underlying material being plastics, pipes are produced in a wending process such that small variations in the material cause continuous variations of λ along the pipe). Moreover, they have to be connected either by a screw system or welding and the connections itself may introduce jump discontinuities to a spatially varying friction coefficient. As a consequence, a pipe-wise constant friction coefficient can merely be seen as approximation to a pipe-wise distributed one.

To the best of our knowledge, the identification of the friction coefficient as a function depending on the spatial dimension is still an open problem. We mention, however, that in [5], a model somewhat related to (2) was investigated where the nonlinear source term was replaced by a function depending on velocity only. The function was identified for a single pipe in the context of semigroup solutions to the system. Problems related to limited knowledge on the initial data were avoided by choosing a specific steady state of the system with zero mass flow and constant pressure.

The rest of this paper is organized as follows. In Section 2 the notion of broad solutions to semilinear systems of conservation laws in case of networks of pipelines for the transport of natural gas is introduced. In Section 3, the existence of broad solutions for the problem under investigation is established in the stationary and time-dependent setting. Moreover, sensitivity properties of the solutions to (2) with respect to variations of λ are obtained. Section 4 introduces the identification problem in an output-least-squares formulation and establishes the existence of solutions under suitable assumptions. Finally, Section 5 validates the theoretical findings by numerical experiments.

Notation: In this paper $\Omega \subset \mathbb{R}^1$ denotes the spatial domain for the partial differential system. In case of a network, Ω consists of disjoint intervals each of which representing a specific pipe. The time-space cylinder is denoted by $\mathcal{Q} = (0, T) \times \Omega$. By $L^p(\cdot)$, with $1 \leq p \leq \infty$, we denote the usual Lebesgue spaces and $\mathbf{L}^\infty(\mathcal{Q}) := (L^\infty(\mathcal{Q}))^2$. To shorten notation, expressions of the form $(F)[x]$ correspond to the evaluation of the functions appearing in F at the argument x. A typical example would be $F = \frac{q|q|}{\rho}$. An index appearing in parenthesis, $(i), i \in \mathbb{N}$, relates the variable to

pipeline i. Finally, we utilize the abbreviation $c_a := (1+a^2)^{-\frac{1}{2}}$.

2. Preliminaries. The state system (2) can be written as

$$y_t + Ay_x = g(y), \tag{3}$$

with $y := (\rho, q)^\top$ denoting the state vector. Here $g(y)$ and the A are defined by

$$g(y) = (0, -\lambda \tfrac{q|q|}{\rho})^\top \text{ and } A = \begin{pmatrix} 0 & 1 \\ a^2 & 0 \end{pmatrix}.$$

The eigenvalues of A, given by $\sigma_1 = -a < a = \sigma_2$, define *characteristic lines*. Indeed, given a position $x \in (x_L, x_R)$ and a point in time $\tau \in (0,T)$, the characteristics passing through (τ, x) are defined as solutions to the ordinary differential equations

$$\dot{s}_i(t;\tau,t) = \sigma_i$$

with $s_i(\cdot;\tau,x) : \mathbb{R} \to \mathbb{R}$ satisfying $s_i(\tau;\tau,x) = (\tau,x)$. The index i relates characteristic and eigenvalue. Since the domain $\mathcal{Q}$ is bounded, we define the times $\underline{t}_i(\tau,x) \in [0,\tau]$ and $\bar{t}_i(\tau,x) \in [\tau,T]$, specifying the time, the i-th characteristic passing through (τ,x) satisfies $(t, s_i(t;\tau,x)) \in \mathcal{Q}$, i.e., we either have $s_i(\underline{t}_i(\tau,x);\tau,x) = x, x \in [x_L, x_R]$ in case the characteristic intersects with $\{0\}\times[x_L,x_R]$ or $s_1(\underline{t}_1(\tau,x);\tau,x) = x_R$ or $s_2(\underline{t}_2(\tau,x);\tau,x) = x_L$ if the characteristic intersects with the boundary $(0,T)\times\{x_R\}$ or $(0,T)\times\{x_L\}$, respectively. The time $\bar{t}_i(\tau,x)$ is defined correspondingly.

Based on a transformation of the representation (3), we consider *broad solutions* for (2) as follows. Due to strict hyperbolicity of (2), there exist a matrix $L \in \mathbb{R}^{n\times n}$ such that $A = LDL^{-1}$ where $D = diag(\sigma_i) \in \mathbb{R}^{2\times 2}$. Multiplying (3) from the left by L^{-1}, using the linearity of differentiation and setting $\mathcal{T}(y) := L^{-1}y$ and $f(y) := L^{-1}g(y)$, we obtain

$$(\mathcal{T}(y))_t + D(\mathcal{T}(y))_x = f(y),$$

a system of scalar, linear transport equations, merely coupled by the source term on the right hand side. Given (2), the transformation matrices are

$$L = c_a \begin{pmatrix} 1 & 1 \\ -a & a \end{pmatrix}, \quad L^{-1} = (2c_a)^{-1} \begin{pmatrix} 1 & -a^{-1} \\ 1 & a^{-1} \end{pmatrix}.$$

Note also, that the linear transport equations even have constant coefficients. In case of a single equation of this type, it is well known that solutions are described by ordinary differential equations along the characteristic line, defined by the constant coefficient. The concept of broad solutions extends this property to systems in that the transformed components of $\mathcal{T}(y)$ are absolutely continuous functions along the corresponding characteristic lines. Broad solutions to semilinear systems of balance laws for unbounded domains have been studied for example in [1, 20], while in [10, 11] bounded domains have been considered.

The lateral boundaries of $\mathcal{Q}$ are approached by exactly one of the characteristics for every $t \in (0,T)$. To be able to reconstruct the original variables at the boundary, the matrices

$$C_L = \begin{pmatrix} c_1 \\ c_L \end{pmatrix}^\top, \quad C_R = \begin{pmatrix} c_2 \\ c_R \end{pmatrix}^\top$$

have to be invertible, restricting the possible linear combinations of y that can be prescribed. Here, $c_1, c_2 \in \mathbb{R}^2$ denote the rows of L^{-1}.

So for we have described the modeling of gas transport through a single pipe. In order to extend this to a network of pipes with $N_P \in \mathbb{N}$ pipes and $N_J \in \mathbb{N}$ junctions, we utilize the representation of the network as a directed graph with edges modeling the pipelines $(x_L^{(i)}, x_R^{(i)})$ for $i \in \{1,...,N_P\}$ on each of which the transport equation (2) has to hold. For every node $j \in \{1,...,N_J\}$, there exist index sets n_L^j, n_R^j denoting its ingoing and outgoing edges, respectively.

Besides entry- and exit nodes with only one adjacent pipeline, the internal nodes correspond to points of pipe interaction, i.e. nodes where at least two pipes connect. We only consider passive networks, limiting the pipe interactions to junctions with coupling conditions as follows. On the one hand, the volume flow has to be balanced such that Kirchhoff's circuit law

$$\sum_{i \in n_L^j} q^{(i)}(x_R^{(i)}) + dq_j = \sum_{i \in n_R^j} q^{(i)}(x_L^{(i)}) \tag{4}$$

holds true. Here, dq_j denotes possible injection or extraction of gas at the corresponding node. On the other hand, the pressure has to be conserved, i.e., we require

$$p^{(l)}(x_R^{(l)}) = p_j = p^{(k)}(x_L^{(k)}) \text{ for all } l \in n_L^j \text{ and } k \in n_R^j. \tag{5}$$

These coupling conditions allow for reconstructing the original state variable as the following example demonstrates.

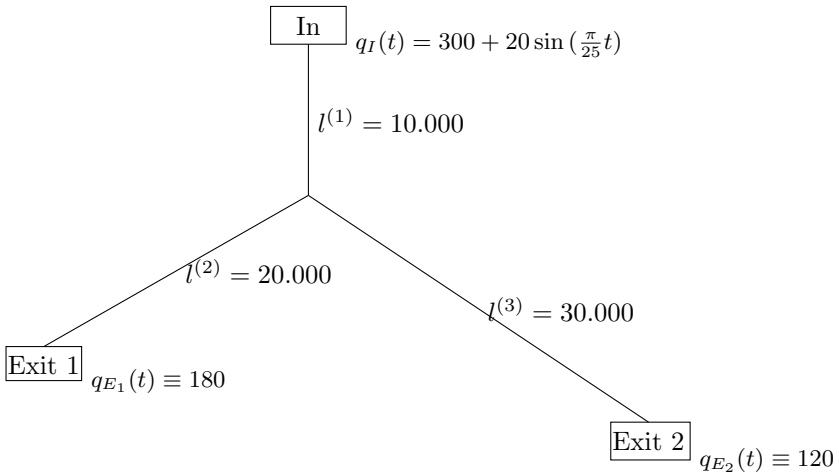

Fig. 1: Sketch of a basic passive Network

EXAMPLE 1. *Consider the internal node of the Y-shaped network consiedred in Example 5 of Section 5 and depicted in Figure 1. Here, $n_L = \{1\}$, $n_R = \{2, 3\}$ and consequently, the second component of $\mathcal{T}$ from pipe 1, $\mathcal{T}_2^{(1)}$ and the first component of $\mathcal{T}$ from pipe 2 and 3, $\mathcal{T}_1^{(2)}$ and $\mathcal{T}_1^{(3)}$, respectively, approach the junction. As a consequence, the original state variables $\{(\rho^{(i)}, q^{(i)})\}_{i=1}^3$ have to satisfy the linear system*

$$\begin{pmatrix} (2c_a)^{-1} & (2c_a a)^{-1} & 0 & 0 & 0 & 0 \\ 0 & 0 & (2c_a)^{-1} & (2c_a a)^{-1} & 0 & 0 \\ 0 & 0 & 0 & 0 & (2c_a)^{-1} & (2c_a a)^{-1} \\ 1 & 0 & -1 & 0 & 0 & 0 \\ 1 & 0 & 0 & 0 & -1 & 0 \\ 0 & 1 & 0 & -1 & 0 & -1 \end{pmatrix} \begin{pmatrix} \rho^{(1)} \\ q^{(1)} \\ \rho^{(2)} \\ q^{(2)} \\ \rho^{(3)} \\ q^{(3)} \end{pmatrix} = \begin{pmatrix} \mathcal{T}_2^{(1)} \\ \mathcal{T}_1^{(2)} \\ \mathcal{T}_1^{(2)} \\ 0 \\ 0 \\ 0 \end{pmatrix} \tag{6}$$

at the junction and $\mathcal{T}_1^{(1)}, \mathcal{T}_2^{(2)}, \mathcal{T}_2^{(3)}$ are obtained as linear combinations of the solution according to the transformation matrix L.

Next, we formally define broad solutions.

DEFINITION 1. *A broad solution of (2) is a function $y = L\mathcal{T}(y) : \mathcal{Q} \to \mathbb{R}^2$ such that for almost every $(\tau, x) \in \mathcal{Q}$, the map $t \mapsto \mathcal{T}_i(y)[t, s_i(t; \tau, x)]$ is an absolutely continuous function satisfying*

(i) at almost every $(\tau, x) \in \mathcal{Q}$ *the ordinary differential equations*

$$\frac{d}{dt}\mathcal{T}_i(y)[t, s_i(t;\tau,x)] = f_i(t, s_i(t;\tau,x), y(t, s_i(t;\tau,x))) \tag{7}$$

almost everywhere on $(\underline{t}_i(\tau,x), \overline{t}_i(\tau,x))$ *for* $i = 1, 2$,

(ii) the initial condition at $x \in (x_L, x_R)$

$$\mathcal{T}_i(y)[0,x] = c_i y_0(x),$$

(iii) the boundary condition at x_L *in the sense that for almost every* $t \in (0,T)$ *we have*

$$\mathcal{T}_2(y)[t,x_L] = c_2 C_L^{-1} \begin{pmatrix} \mathcal{T}_1(y)[t,x_L] \\ d_L(t) \end{pmatrix},$$

(iv) the boundary condition at x_R *in the sense that for almost every* $t \in (0,T)$ *we have*

$$\mathcal{T}_1(y)[t,x_R] = c_1 C_R^{-1} \begin{pmatrix} \mathcal{T}_2(y)[t,x_R] \\ d_R(t) \end{pmatrix},$$

(v) in case of a network, (i) and (ii) hold on the pipes $k \in \{1,\dots,N_P\}$*, (iii) and (iv) are satisfied at entry- and exit nodes (see page 4) and the coupling conditions* (4) *and* (5) *are satisfied at the interior nodes* $j \in \{1,...,N_J\}$ *of the network.*

We aim for identifying the friction coefficient λ based on measurements of the pressure, and due to the choice $p(\rho) = a^2\rho$ also of the density. Thus, we impose boundary conditions for the volume flow at the entry- and exit nodes of the network and set

$$c_L := (0,1)^\top, \quad c_R := (0,1)^\top.$$

Besides characteristics we further consider integral curves γ_i. The latter objects are an essential tool for analyzing the behavior of solutions of the underlying transportation process. Each γ_i basically is an extension of s_i to the entire time interval $[0,\tau]$ consisting of all paths along characteristic lines that affect the value of $y(\tau,x)$. In case of (2), formulated on a single pipe, they are formed by the original characteristics s_i on the interval $(\underline{t}_i(\tau,x)),\tau)$. On the interval $(\underline{t}_{\hat{i}}(\underline{t}_i(\tau,x),x_{L/R}),\underline{t}_i(\tau,x))$, they are formed by the other characteristic $s_{\hat{i}}$ ($\hat{i} \in \{1,2\}\backslash\{i\}$) and this alternation repeats until $t = 0$. The index of the integral curves corresponds to the characteristics that actually pass through (τ,x). In case of systems larger than 2×2 or networks with certain coupling conditions, these objects become more complex as they might be multivalued due to interaction with internal nodes.

3. Existence of solutions to the state system (2)**.** After introducing the concept of broad solutions we now establish the existence of such solutions in case of (2). Note that the system has to be closed by boundary conditions, involving data that are observable at the corresponding nodes, and initial conditions. As discussed in Section 1, distributed information on density and volume flow within the closed pipes at fixed times are hardly available, rendering the question for initial data nontrivial. This can be overcome by either additionally identifying the initial data, increasing the complexity of the identification problem significantly, or using initial states that can be described by data that are readily available. In this paper we employ the latter strategy, utilizing steady states of the underlying physical system as initial data. As a consequence, we first study steady states and their dependency on the friction coefficient λ.

The basic regularity assumption for the friction coefficient is $\lambda \in L^1(\Omega)$. Moreover, we assume the existence of a suitable upper bound

$$\|\lambda\|_{L^1(\Omega)} \le \overline{\lambda}. \tag{8}$$

to be specified later.

3.1. Characterization of Steady States. On a single pipe, steady states are formally defined by assuming the derivative of ρ, q with respect to time to be zero, providing the system of ordinary differential equations

$$\tfrac{dq_0}{dx} = 0, \quad \tfrac{d\rho_0}{dx} = -\lambda \frac{q_0|q_0|}{a^2\rho},$$

with associated solutions

$$q_0 = c, \quad \rho_0(x) = \sqrt{\rho(x_L)^2 - 2(\Lambda(x) - \Lambda(x_L))\frac{c|c|}{a^2}}, \tag{9}$$

i.e. they are determined by $\Lambda(x) = \int_{x_L}^{x} \lambda(\tau)d\tau$ and the values for the constant volume flow, $c \in \mathbb{R}$, and the value of the density at the node x_L, $\rho(x_L)$. Both quantities are observable at node x_L. The function $\Lambda(x)$ denotes the absolutely continuous function whose derivative is given by the friction coefficient λ. In case of a passive network, the steady states on each pipeline have to satisfy in addition the coupling conditions (6). In general, this requires knowledge on the steady volume flow q on each pipeline as well as the value of the density ρ at a single point within the network in the context of nomination validation. Determining a feasible steady state in form of (9) for networks has been the subject of active research in the last decades [14, 7] and, by now, efficient algorithms are available (see e.g. [7]).

The following result demonstrates that the (9) indeed represent a steady state for passive networks in the sense of broad solutions.

PROPOSITION 2. *The functions $\rho(t,x) = \rho_0(x), q(t,x) = q_0(x)$ with ρ_0, q_0 given in (9) satisfying, in case of passive networks, the coupling conditions (4) and (5), define a steady state broad solutions, with the latter according to Definition 1.*

Proof. We first prove, that for a given spatial position x in the network, the transformed variables are constant with respect to time. For this purpose, we utilize the identity

$$\begin{aligned}
&-\tfrac{1}{a}\int_{t_1}^{t_2} \lambda(x_L + a\tau)\frac{\frac{c|c|}{a^2}}{\sqrt{\rho(x_L)^2 - 2\Lambda(x_L+a\tau)\frac{c|c|}{a^2}}}dx \\
=&\sqrt{\rho(x_L)^2 - 2\Lambda(x_L+at_2)\frac{c|c|}{a^2}} - \sqrt{\rho(x_L)^2 - 2\Lambda(x_L+at_1)\frac{c|c|}{a^2}}
\end{aligned}$$

and the characteristics s_1, s_2. Given an initial condition with volume flows $q^{(i)} \equiv c^{(i)}$, friction coefficients $\lambda^{(i)}(x)$ and corresponding densities $\rho_0^{(i)}(x)$ satisfying the coupling conditions (4) and (5), we first consider boundary nodes of a fixed pipe i in the network. Let $0 < \Delta t \leq \overline{T} = \min_{i\in 1,\dots,N_P} \frac{|x_R^{(i)} - x_L^{(i)}|}{a}$ be a time increment ensuring, that $s_{1/2}(0;\Delta t, x_{L/R}^{(i)})$ is contained in pipe i. Recall that $x_L^{(i)}$ is approached by the first characteristic while $x_R^{(i)}$ is approached by the second. The chosen notation allows for the simultaneous treatment of both cases. We find

$$\begin{aligned}
\mathcal{T}_{1/2}^{(i)}(\Delta t, x_{L/R}^{(i)}) =&(2c_a)^{-1}\left(\rho_0^{(i)}(x_{L/R}^{(i)} \pm a\Delta t) \mp a^{-1}c^{(i)}\right) \\
&\pm (2ac_a)^{-1}\int_0^{\Delta t} \lambda^{(i)}(x_{L/R}^{(i)} \pm a(\Delta t - \tau))\frac{c^{(i)}|c^{(i)}|}{\rho_0^{(i)}(x_{L/R}^{(i)} \pm a(\Delta t-\tau))}d\tau \\
=&(2c_a)^{-1}\left(\rho_0^{(i)}(x_{L/R}^{(i)} \pm a\Delta t) \mp a^{-1}c^{(i)} + \rho_0^{(i)}(x_{L/R}^{(i)}) - \rho_0^{(i)}(x_{L/R}^{(i)} \pm a\Delta t)\right) \\
=&\mathcal{T}_{1/2}^{(i)}(0, x_{L/R}^{(i)}).
\end{aligned}$$

Recovering the original states at interior, entry- and exit nodes of the network is based on solving linear systems where the right hand side is given by the transformed variables that approach the corresponding nodes and possible boundary conditions (see (iii)-(v) in Definition 1). In particular,the boundary conditions are constant over time as we consider a steady state and consequently,

the right hand sides of the linear systems and thus their solutions, are constant over time. Based on this observation, we establish

$$\mathcal{T}_{1/2}^{(i)}(\Delta t, x) = \mathcal{T}_{1/2}^{(i)}(0, x)$$

for an arbitrary position x by following the integral curves $\gamma_{1/2}(\cdot; \Delta t, x)$ and using the transformation in (ii) of Definition 1 and (7). Finally, this implies $\rho^{(i)}(t,x) = \rho_0^{(i)}(x)$ and $q^{(i)}(t,x) = c$ for all $x \in (x_L^{(i)}, x_R^{(i)})$ and $i = 1, ..., N_P$. Consequently, the steady state forms a broad solution of (2) in the sense of Definition 1. ∎

Considering steady states in the network and measurements of the corresponding pressure at nodes only, the identification of a distributed friction coefficient $\lambda = \lambda(x)$ in the pipes is not possible. Indeed, the difference of the squared densities at $x_L^{(i)}, x_R^{(i)}$ is given by

$$\rho(x_R^{(i)})^2 - \rho(x_L^{(i)})^2 = -2(\Lambda(x_R^{(i)}) - \Lambda(x_L^{(i)}))\frac{c|c|}{a^2}. \tag{10}$$

Note that this difference is realized by all $\tilde{\lambda}$ with $\int_{x_L}^{x_R} \tilde{\lambda}(x)dx = (\Lambda(x_R^{(i)}) - \Lambda(x_L^{(i)}))$. Moreover, such problems arise for pipewise constant friction coefficients in the case of networks as well. Here, the identification is possible, if at least as many steady states of the network are evaluated as pipes are in the longest path from one measurement device to the next. However, numerical experiments suggest, that this identification process is well-defined in the time dependent setting.

Since the steady states directly depend on the friction coefficient, we will next analyze this relationship on a single pipe.

PROPOSITION 3. *Consider a fixed value c for the steady volume flow q and let the friction coefficient satisfy*

$$\|\lambda\|_{L^1(x_L,x_R)} \leq \tfrac{1}{2}\left(\tfrac{\rho(x_L)a}{c}\right)^2 - \varepsilon \tag{11}$$

for $0 < \varepsilon << 1$. Then the steady state of the density depends locally Lipschitz continuous on λ such that for all $\tilde{\lambda}$ with $\|\tilde{\lambda}\| \leq \frac{1}{2}\left(\frac{\rho(x_L)a}{c}\right)^2 - \tilde{\varepsilon}$ with $0 < \tilde{\varepsilon} \leq \varepsilon$ we have

$$\|\rho_0(\lambda) - \rho_0(\tilde{\lambda})\|_{L^\infty(x_L,x_R)} \leq K(\varepsilon')\|\lambda - \tilde{\lambda}\|_{L^1(x_L,x_R)}.$$

Moreover, it is twice Fréchet differentiable with respect to the friction coefficient. Let h, n denote perturbations with $\|h\|_{L^1(x_L,x_R)}, \|n\|_{L^1(x_L,x_R)}$ sufficiently small. Then the first and second order derivatives are given by

$$\rho_0'(\lambda)[h][x] = -\frac{c|c|}{a^2\rho_0(x)}(H(x) - H(x_L)), \tag{12}$$

$$\rho_0''(\lambda)[h,\mu][x] = -\frac{c^4}{a^4\rho_0}(H(x) - H(x_L))(N(x) - N(x_L)), \tag{13}$$

respectively, with $H(x) = \int_{x_L}^x h(\tau)d\tau$ and $N(x) = \int_{x_L}^x n(\tau)d\tau$.

Proof. Consider some λ satisfying (11), i.e. the density satisfies $\rho_0(\lambda) \geq \sqrt{\varepsilon}$ and is well defined along the pipe. Then there exists a $L^1(x_L, x_R)$-neighborhood $\mathcal{U}$ such that $\rho_0(\tilde{\lambda}) \geq \sqrt{\tilde{\varepsilon}} > 0$ for all $\tilde{\lambda} \in \mathcal{U}$. By the particular expression for the steady density given in (9), for any $x \in [x_L, x_R]$ we find

$$\begin{aligned}
|\rho_0(\tilde{\lambda})[x] - \rho_0(\lambda)[x]| &= \left|\int_{x_L}^x \int_0^1 \tfrac{d}{dl}\rho_0(\lambda - l(\tilde{\lambda} - \lambda))[\xi]dld\xi\right| \\
&= \left|\int_{x_L}^x (\rho_0(\lambda - l(\tilde{\lambda} - \lambda))[\xi])^{-1}\tfrac{c|c|}{a^2}(\tilde{\Lambda}(\xi) - \Lambda(\xi))d\xi\right| \\
&\leq \tfrac{x_R - x_L}{\sqrt{\tilde{\varepsilon}}}\tfrac{|c|^2}{a^2}\|\tilde{\lambda} - \lambda\|_{L^1(\Omega)}
\end{aligned}$$

and thus obtain local Lipschitz continuity. Here we employed the notation outlined in Section 1, i.e., the density that depends on the friction coefficient, $\rho(\lambda)$ is evaluated at position x. Similar estimates for $\rho_0(\lambda + h) - \rho_0(\lambda) - \rho_0'(\lambda)[h]$ and $\rho_0'(\lambda + n)[h] - \rho_0'(\lambda)[h] - \rho_0''(\lambda)[h, n]$ prove the differentiability results. ∎

By linearity of the coupling conditions, the latter result can readily be extended to passive networks. However, to define a steady state on the network, we need a set of constant volume flow rates, each defined on one pipe and satisfying the nodal balancing conditions (4). In addition, the pressure/density has to be defined at one point. Then by (5) and the explicit formula (9), the corresponding pressure/density distribution can be computed. In this case, the derivative of the initial condition on any fixed pipe i not only depends on the variation of $\lambda^{(i)}$, but also on the variations of $\lambda^{(j)}$ on all pipes j that are 'upstream' with respect to the point, where the pressure is fixed, since they have impact on $p(x_L^{(i)})$.

The following example demonstrates this fact.

EXAMPLE 2. *Consider the small passive network depicted in Figure 1 with counter-clock wise numbered pipelines beginning with the one, connected to the entry-node. Let the friction coefficient be pipewise constant with values* $\lambda = (0.02, 0.02, 0.02)$. *The steady state is defined by the pipewise constant volume flows* $q = (300, 120, 180)$, *clearly satisfying* (4), *and a fixed density* $\rho(x_{In}) = 50$. *As a consequence, the steady densities are given by*

$$\begin{aligned}
\rho^{(1)}(x) &= \sqrt{50^2 - 2 \cdot \lambda^{(1)} \cdot \tfrac{300^2}{a^2} x}, \\
\rho^{(2)}(x) &= \sqrt{\rho^{(1)}(l^{(1)})^2 - 2 \cdot \lambda^{(2)} \cdot \tfrac{120^2}{a^2} x}, \\
\rho^{(3)}(x) &= \sqrt{\rho^{(1)}(l^{(1)})^2 - 2 \cdot \lambda^{(3)} \cdot \tfrac{180^2}{a^2} x}.
\end{aligned}$$

For $h = (1, 0, 0)$, *the derivative is given by*

$$\rho_0'^{(1)}[h][x] = -\frac{300^2 x}{a^2 \rho^{(1)}(x)}, \quad \rho_0'^{(2)}[h][x] = -\frac{300^2}{a^2 \rho^{(2)}(x)} l^{(1)}, \quad \rho_0'^{(3)}[h][x] = -\frac{300^2}{a^2 \rho^{(3)}(x)} l^{(1)}.$$

Here, although the second and third component of λ *are not considered, the derivatives of the steady state on the corresponding pipes are non-zero because the friction coefficient on the first pipeline, that is 'upstream', is perturbed.*

Proposition 3 also fixes the upper bound $\overline{\lambda}$ in (8). Here, the value has to be chosen such that the steady state is uniformly strictly positive.

3.2. Transient Solutions. In general, the existence of broad solutions to semilinear systems of balance laws with globally Lipschitz continuous source terms on unbounded domains is based on Banach's Fixed Point Theorem related to the transformed state variables. To enable the fixed point argument, the norm of this Banach space is carefully chosen and depends strongly on the global Lipschitz constant of the source term with respect to the original state variables. Since the source term in (2) is locally Lipschitz continuous only, results from [1, 10] cannot be applied directly and solutions can only be shown to exist for a finite, possibly small, terminal time T (see [1]). Before providing the existence result for solutions to (2), we introduce and justify certain bounds on the state y, that are assumed to hold in the initial condition and for which a global Lipschitz constant of the source term is available. For this purpose, the density ρ is assumed to be uniformly positive, i.e. there has to exist some $\underline{\rho}$ with

$$\rho \geq \underline{\rho} > 0 \text{ on } \Omega. \tag{14}$$

This assumption is aimed to avoid vacuum states in the solution of (2), appearing to impose a minor constraint in real world gas transport only. Moreover, we assume the pressure in the pipes to be bounded as otherwise one may assume damage of a pipe. Let $\overline{p}$ denote an upper bound.

According to the chosen pressure law, this directly translates into an upper bound for the density of the form

$$\rho \leq \overline{\rho} := a^{-2}\overline{p} \text{ on } \Omega. \tag{15}$$

The volume flow is assumed to be bounded as well, i.e. there exists $\overline{q} > 0$ such that

$$|q| \leq \overline{q} \text{ on } \Omega. \tag{16}$$

This is justified by properties of the nonlinear system (1). In this case, the eigenvalues of the Jacobian of the flux function are given by $\sigma_1 = \rho^{-1}q - a$ and $\sigma_2 = \rho^{-1}q + a$, i.e., they have different signs in case of $\rho^{-1}q = v < a$ only. In other words, in subsonic regimes, where transport speed v is lower than the speed of sound a. Since the sign structure of the eigenvalues is essential for the imposition of boundary conditions to the system, we restrict ourselves to the setting $\sigma_1 < 0 < \sigma_2$, i.e., we assume the velocity $v = \rho^{-1}q$ to be bounded by a. Using (14) and (15) we obtain

$$|q| = |v\rho| \leq a\overline{\rho} = \overline{q}.$$

Under these conditions we can establish the existence of broad solutions of the underlying system.

The following result establishes the existence of broad solutions for the very general case of initial and boundary data that are merely essentially bounded. For this purpose, the initial and boundary data have to satisfy conditions that not only guarantee pointwise feasibility with respect to (14)-(16) for themselves, but also for weighted averages in certain neighborhoods, with averages depending on the transformed variables.

PROPOSITION 4. *Let a passive network of pipelines be given. Let initial and boundary data be given such that there exists a radius $r > 0$ and*

(i) every pipeline i is covered with open balls

$$B_r(x_k) \text{ with } x_k := \min\{x_L^{(i)} + kr, x_R^{(i)}\}, k = 0, ..., \left\lceil \tfrac{x_R^{(i)} - x_L^{(i)}}{r} \right\rceil =: K,$$

(ii) for all $k \in \{0, ..., K\}$ and $x, \hat{x} \in B_r(x_k) \cap [x_L^{(i)}, x_R^{(i)}]$, (ρ, q) reconstructed from $\mathcal{T}(y)[0, x]$ and $\mathcal{T}(y)[0, \hat{x}]$ are strictly feasible with respect to (14)-(16), i.e., for $x \leq \hat{x}$ we have

$$\underline{\rho} < c_a(\mathcal{T}_1(y)[0, \hat{x}] + \mathcal{T}_2(y)[0, x]) < \overline{\rho},$$
$$|c_a a(\mathcal{T}_2(y)[0, x] - \mathcal{T}_1(y)[0, \hat{x}])| < \overline{q},$$

(iii) for all entry- and exit nodes j we have for pipeline $i \in n_R^j$ and $x, \hat{x} \in B_r(x_L^{(i)})$, $x - x_L^{(i)} \leq \frac{r}{2}, x < \hat{x}$,

$$\underline{\rho} < c_a(\mathcal{T}_1(y)[0, \hat{x}] + \mathcal{T}_1(y)[0, x] + \tfrac{1}{c_a a} d_j(a^{-1}(x - x_L^{(i)}))) < \overline{\rho},$$
$$|c_a a(\mathcal{T}_1(y)[0, \hat{x}] + \mathcal{T}_1(y)[0, x] + \tfrac{1}{c_a a} d_j(a^{-1}(x - x_L^{(i)})))| < \overline{q},$$

and for pipeline $i \in n_L^j$, $x, \hat{x} \in B_r(x_R^{(i)})$, $x < \hat{x}, x_R^{(i)} - \hat{x} \leq \frac{r}{2}$, that

$$\underline{\rho} < c_a(\mathcal{T}_2(y)[0, x] + \mathcal{T}_2(y)[0, \hat{x}] + \tfrac{c_a}{a} d_j(a^{-1}(x_R^{(i)} - \hat{x}))) < \overline{\rho},$$
$$|c_a a(\mathcal{T}_2(y)[0, x] + \mathcal{T}_2(y)[0, \hat{x}] + \tfrac{c_a}{a} d_j(a^{-1}(x_R^{(i)} - \hat{x})))| < \overline{q},$$

respectively,

(iv) for all junctions j, we have for all pipelines $i \in n_R^j$, $x \in B_r(x_L^{(i)})$ and $x - x_L^{(i)} < \frac{r}{2}$, that $\mathcal{T}_2^{(i)}(a^{-1}(x - x_L^{(i)}), x_L^{(i)})$ reconstructed from $\mathcal{T}_1^l(0, x_L^l + (x - x_L^{(i)}))$, $l \in n_R^j$, and $\mathcal{T}_2^l(0, x_R^{(l)} - (x - x_L^{(i)}))$, $l \in n_L^j$, satisfy, with $\hat{x} \in B_r(x_L^{(i)}), x < \hat{x}$,

$$\underline{\rho} < c_a(\mathcal{T}_1(y)[0, \hat{x}] + \mathcal{T}_2(y)[0, a^{-1}(x - x_L^{(i)})]) < \overline{\rho},$$
$$|c_a a(\mathcal{T}_2(y)[0, a^{-1}(x - x_L^{(i)})] - \mathcal{T}_1(y)[0, \hat{x}])| < \overline{q},$$

and all pipelines $i \in n_L^j$, $x \in B_r(x_R^{(i)})$ *and* $x_R^{(i)} - x < \frac{r}{2}$, *that* $\mathcal{T}_1^{(i)}(a^{-1}(x_R^{(i)} - x), x_R^{(i)})$ *reconstructed from* $\mathcal{T}_1^{(l)}(0, x_L^{(l)} + (x - x_L^{(i)}))$, $l \in n_R^j$, *and* $\mathcal{T}_2^{(l)}(0, x_R^{(l)} - (x - x_L^{(i)}))$, $l \in n_L^j$, *satisfy, with* $\hat{x} \in B_r(x_R^{(i)}), \hat{x} < x$,

$$\begin{aligned}\underline{\rho} < c_a(\mathcal{T}_1^{(i)}(y)[a^{-1}(x_R^{(i)} - x), x_R^{(i)}] + \mathcal{T}_2^{(i)}(y)[0, \hat{x}]) < \overline{\rho},\\ |c_a a(\mathcal{T}_2^{(i)}(y)[0, \hat{x}] - \mathcal{T}_1^{(i)}(y)[a^{-1}(x_R^{(i)} - x), x_R^{(i)}])| < \overline{q},\end{aligned}$$

respectively.

Then, there exists a time T *such that the initial-boundary value problem* (2), (IC), (BC) *admits a unique broad solution* $y \in \mathbf{L}^\infty(\mathcal{Q})$ *satisfying* (14)-(16) *for* λ *according to* (8).

Proof. The proof is based on a fixed point argument (as in [1] for unbounded domains) but accounts for bounded domains with corresponding boundary conditions (as in [10]). Without loss of generality, it considers $T \leq \overline{T}/2$ with $\overline{T}$ as defined in the proof of Proposition 2. Then the results can be extended to larger times by a bootstrapping argument. Since the source term is merely locally Lipschitz continuous with respect to the state variables (ρ, q), it is first shown that, if initial and boundary data satisfy assumptions (i)-(iv) and λ satisfies (8), then there exists a time $T > 0$, such that a broad solution, if it exists, satisfies the bounds (14)-(16). Here, the time T only depends on the bounds $\overline{\rho}, \underline{\rho}, \overline{q}, \overline{\lambda}$ and the radius r.

To establish this result, we fix a pipeline i and provide estimates for the state variables $(\rho^{(i)}, q^{(i)})[\tau, x]$ for almost every (τ, x) with $x \in [x_L^{(i)}, x_R^{(i)}]$ and $0 < \tau \leq a^{-1}\frac{r}{2}$, based on the integral curves.

Recall that the original state variables are recovered from the transformed variables by $L\mathcal{T}$ and thus they are given by

$$\begin{aligned}\rho^{(i)}(\tau, x) &= c_a(\mathcal{T}_1^{(i)}(y)[\tau, x] + \mathcal{T}_2^{(i)}(y)[\tau, x]),\\ q^{(i)}(\tau, x) &= c_a a(\mathcal{T}_2^{(i)}(y)[\tau, x] - \mathcal{T}_1^{(i)}(y)[\tau, x]).\end{aligned} \tag{17}$$

Moreover, the values of $\mathcal{T}_1^{(i)}(\tau, x), \mathcal{T}_2^{(i)}(\tau, x)$ are given by

$$\begin{aligned}\mathcal{T}_1^{(i)}(y)[\tau, x] = \mathcal{T}_1^{(i)}(y)[\underline{t}_1(\tau, x), x + a(\tau - \underline{t}_1(\tau, x))]\\ + \tfrac{c_a^{-1}}{2a} \int_{\underline{t}_1(\tau,x)}^{\tau} \lambda(x + a(\tau - t))\tfrac{q|q|}{\rho}[t, x + a(\tau - t)]dt,\\ \mathcal{T}_2^{(i)}(y)[\tau, x] = \mathcal{T}_2^{(i)}(y)[\underline{t}_2(\tau, x), x - a(\tau - \underline{t}_2(\tau, x))]\\ - \tfrac{c_a^{-1}}{2a} \int_{\underline{t}_2(\tau,x)}^{\tau} \lambda(x - a(\tau - t))\tfrac{q|q|}{\rho}[t, x - a(\tau - t)]dt.\end{aligned}$$

Consequently, we obtain

$$\begin{aligned}\rho^{(i)}(\tau, x) &= c_a(\mathcal{T}_1^{(i)}(y)[\tau, x] + \mathcal{T}_2^{(i)}(y)[\tau, x])\\ &= c_a(\mathcal{T}_1^{(i)}(y)[\underline{t}_1(\tau, x), x + a(\tau - \underline{t}_1(\tau, x))] + \mathcal{T}_2^{(i)}(y)[\underline{t}_2(\tau, x), x - a(\tau - \underline{t}_2(\tau, x))])\\ &\quad + \tfrac{1}{2a} \int_{\underline{t}_1(\tau,x)}^{\tau} \lambda(x + a(\tau - t))\tfrac{q^{(i)}|q^{(i)}|}{\rho^{(i)}}[t, x + a(\tau - t)]dt\\ &\quad - \tfrac{1}{2a} \int_{\underline{t}_2(\tau,x)}^{\tau} \lambda(x - a(\tau - t))\tfrac{q^{(i)}|q^{(i)}|}{\rho^{(i)}}[t, x - a(\tau - t)]dt,\end{aligned}$$

and analogously an expression for $q^{(i)}(\tau, x)$. The time-space cylinder of the pipeline is depicted in Figure 2 and separated in areas *I-III* by the characteristics emanating from $\{0\} \times x_L^{(i)}$ and $\{0\} \times x_R^{(i)}$.

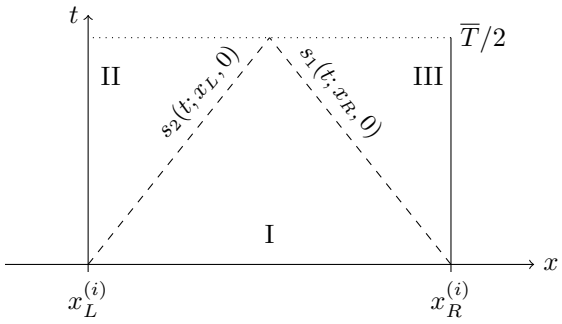

Fig. 2: Phase space.

For $(\tau, x) \in I$ we have $\underline{t}_1(\tau, x) = \underline{t}_2(\tau, x) = 0$ and, by assumption (i), there exists some x_k such that $x + a\tau, x - a\tau \in B_r(x_k)$. The integrals in the representation of $\rho^{(i)}(\tau, x)$ can be estimated by

$$-\tfrac{1}{a}\tau\overline{\lambda}\tfrac{\overline{q}^2}{\underline{\rho}} \leq \tfrac{1}{2a}\int_0^\tau \lambda(x + a(\tau - t))\tfrac{q^{(i)}|q^{(i)}|}{\rho^{(i)}}[t, x + a(\tau - t)]dt$$
$$-\tfrac{1}{2a}\int_0^\tau \lambda(x - a(\tau - t))\tfrac{q^{(i)}|q^{(i)}|}{\rho^{(i)}}[t, x - a(\tau - t)]dt \leq +\tfrac{1}{a}\tau\overline{\lambda}\tfrac{\overline{q}^2}{\underline{\rho}}.$$

Similar estimates can be established for $|q^{(i)}(\tau, x)|$ and as a consequence of assumption (ii), $\underline{\rho} < c_a(\mathcal{T}_1^{(i)}(y)[0, x + a\tau] + \mathcal{T}_2^{(i)}(y)[0, x - a\tau]) < \overline{\rho}$ and $|c_a a(\mathcal{T}_2^{(i)}(y)[0, x - a\tau] - \mathcal{T}_1^{(i)}(y)[0, x + a\tau])| < \overline{q}$ for τ sufficiently small. This provides

$$\underline{\rho} \leq \rho(\tau, x) \leq \overline{\rho}, \quad |q(\tau, x)| \leq \overline{q} \text{ for all } (\tau, x) \in I \cap ((0, T) \times (x_L^{(i)}, x_R^{(i)}))$$

for T sufficiently small. Assumptions (iii) and (iv) allow for similar estimates in case of $(\tau, x) \in II$ or $(\tau, x) \in III$ and $x_L^{(i)}$ or $x_R^{(i)}$ being an entry- or exit-node with corresponding boundary data, or a junction, respectively. This shows that there exists a $T > 0$ such that $y(\tau, x)$ satisfies the bounds for $\tau \in (0, T)$, $x \in \Omega$ and all λ satisfying (8).

Secondly, we establish the existence of broad solutions employing Banach's Fixed-Point Theorem. For this purpose let

$$\tfrac{2}{c_a a}\max\{\tfrac{\overline{q}}{2\underline{\rho}}, (\tfrac{\overline{q}}{\underline{\rho}})^2\} =: L_f \tag{18}$$

denote the Lipschitz constant of $\frac{1}{c_a a}\frac{q|q|}{\rho}$ with respect to $|y|_{l^\infty}$, fix a pipeline i and consider $(\tau, x) \in (0, T) \times \Omega$. In case of $(\tau, x) \in I$, the mapping $\mathcal{T}(y)$ is defined as

$$\mathcal{T}_j(y)[\tau, x] := c_j(\rho_0^{(i)}, q_0^{(i)})[s_j(0; \tau, x)] + \int_0^\tau f_j(t, s_j(t; \tau, x), y(t, s_j(t; \tau, x)))dt \text{ for } j = 1, 2,$$

while, in case of $(\tau, x) \in II$, we have

$$\mathcal{T}_1(y)[\tau, x] := \mathcal{T}_1(y)[\underline{t}_1(\tau, x), x_L^{(i)})] + \int_{\underline{t}_1(\tau,x)}^\tau f_1(t, s_1(t; \tau, x), y(t, s_1(t; \tau, x)))dt,$$

and for $(\tau, x) \in III$

$$\mathcal{T}_2(y)[\tau, x] := \mathcal{T}_2(y)[\underline{t}_2(\tau, x), x_R^{(i)}] + \int_{\underline{t}_2(\tau,x)}^\tau f_2(t, s_2(t; \tau, x), y(t, s_2(t; \tau, x)))dt,$$

respectively. Obviously, $\mathcal{T}(\cdot) : X \to X$ where X denotes the space of essentially bounded functions, equipped with an exponentially weighted sup-norm which is defined as

$$\|\varphi\|_* := \operatorname*{ess\text{-}sup}_{(t,x)\in\mathcal{Q},i=1,2} e^{-2Ct}|\mathcal{T}_i(\varphi)[t,x]|$$

with a constant $C > 0$ to be determined. By $1 \geq e^{-2Ct} \geq e^{-2CT} \forall t \in [0,T]$, this norm is equivalent to $\|\cdot\|_{\mathbf{L}^\infty(\mathcal{Q})}$, rendering $(X, \|\cdot\|_*)$ a Banach space. In the one-pipeline scenario, for any $y, v \in X$ with $\|y - v\|_* = \delta$, we find for $(\tau, x) \in I$ that

$$\begin{aligned}
|\mathcal{T}_i(y)[\tau,x] - \mathcal{T}_i(v)[\tau,x]| &\leq \int_0^\tau |f_i(t, s_i(t;\tau,x), y(t, s_i(t;\tau,x)) - f_i(t, s_i(t;\tau,x), v(t, s_i(t;\tau,x))|dt \\
&\leq \int_0^\tau \overline{\lambda} L_f |y(t, s_i(t;\tau,x)) - v(t, s_i(t;\tau,x))|_{l^\infty} \\
&\leq \int_0^\tau \overline{\lambda} L_f |L|_{l^\infty} |\mathcal{T}_i(y)[t, s_i(t;\tau,x)] - \mathcal{T}_i(v)[t, s_i(t;\tau,x)]|_{l^\infty} \\
&\leq \int_0^\tau \tilde{L}_f \delta e^{2Ct} dt.
\end{aligned}$$

Here, $\tilde{L}_f := \overline{\lambda} L_f |L|_\infty$ combines the bound on λ, (18) and the matrix norm of the transformation matrix L induced by $|\cdot|_{l^\infty}$, taking into account $y = L\mathcal{T}(y)$. Choosing $C = \tilde{L}_f$, integration provides

$$e^{-2\tilde{L}_f \tau} |\mathcal{T}_i(y)[\tau,x] - \mathcal{T}_i(v)[\tau,x]| \leq \frac{1}{2}\delta = \frac{1}{2}\|y - v\|_*$$

almost everywhere in $\mathcal{Q}$. Thus, $\mathcal{T}$ is a contraction on $(X, \|\cdot\|_*)$ with rate $\frac{1}{2}$. To incorporate interactions with boundaries, i.e., considering $(\tau, x) \in II$ or $(\tau, x) \in III$, the contraction property follows analogously, utilizing $f_1(\cdot) = -f_2(\cdot)$ and the fact, that the boundary conditions are independent of the state and cancel out.

In case of passive networks, the constant C has to be increased sufficiently to take into account, that $\mathcal{T}_2(y)[\underline{t}_2(\tau,x), x_L^{(i)})]$ for $i \in n_R^j$ at node j is given as linear combination of $|n_L^j| + |n_R^j|$ transformed variables. In other words,, for every junction j there exists a matrix $c_j \in \mathbb{R}^{(|n_L^j|+|n_R^j|)\times(|n_L^j|+|n_R^j|)}$ with $\mathcal{T}_\rightarrow(t) = c_j \mathcal{T}_\leftarrow(t)$. Here, $\mathcal{T}_\rightarrow(t)$ represents the vector of transformed variables that are emanating from junction j, i.e., $\mathcal{T}_2(t, x_L^{(i)})$ for $i \in n_R^j$ and $\mathcal{T}_1(t, x_R^{(i)})$ for $i \in n_L^j$, and $\mathcal{T}_\leftarrow$ represents the vector of transformed variables entering junction j. Thus, choosing $C = \max_{1\leq j\leq N_J} |c_j|_{l^\infty} \tilde{L}_f$ allows for establishing the same contraction rate as in the one-pipeline scenario in case of a passive network. In part one of the proof we showed that a broad solution has to satisfy the original bounds (14)-(16) if (8) holds true. As a consequence, for T sufficiently small, the fixed point of $\mathcal{T}$ has to be strictly feasible with respect to the bounds, on which the choice of L_f is based on. By

$$\|\cdot\|_X \geq c\|\cdot\|_{\mathbf{L}^\infty(\mathcal{Q})}$$

with $c = c(L_f, T)$, also the pointwise distance to the fixed point is decreasing almost everywhere in $\mathcal{Q}$ in each iteration. Consequently, choosing a feasible initialization of the fixed point iteration ensures that every iterate is feasible with respect to the bounds (14)-(16). ∎

REMARK 1. *Assumptions (ii)-(iv) represent restrictions on possible jumps in initial and boundary condition compared to the distance of the data to the bounds in* (14), (15) *and* (16). *If the initial data for density and volume flow are steady states of the underlying system, the assumptions of Proposition 4 become more specific.*

In fact, fixing a pipeline i and given $x \in [x_L^{(i)}, x_R^{(i)}]$ and $0 < \tau$ such that $(\tau, x) \in I$ from Figure 2, the inequalities in Assumption (ii) become

$$\begin{aligned}
\underline{\rho} < \tfrac{1}{2}(\rho_0^{(i)}(x - a^{-1}\tau) + \rho_0^{(i)}(x + a^{-1}\tau)) < \overline{\rho}, \\
|q^{(i)} + \tfrac{a}{2}(\rho^{(i)}(x - a^{-1}\tau) - \rho^{(i)}(x + a^{-1}\tau))| < \overline{q}.
\end{aligned}$$

In other words, assumption (i) is satisfied concerning density if the initial data obey the upper and lower bound (14), (15) pointwise while the inequality concerning $\overline{q}$ holds for τ sufficiently small, if the constant volume flow $q^{(i)}$ strictly satisfies the bound from (16). For Assumption (iii), the inequalities read as

$$\begin{aligned}\underline{\rho} < \tfrac{1}{2}(\rho_0^{(i)}(2x_L^{(i)} - x + a^{-1}\tau) + \rho_0^{(i)}(x + a^{-1}\tau) + \tfrac{1}{a}(d_j(\tau - a(x - x_L^{(i)})) - q^{(i)}) < \overline{\rho},\\ |d_j(\tau - a(x - x_L^{(i)})) + \tfrac{a}{2}(\rho^{(i)}(2x_L^{(i)} - x + a^{-1}\tau) - \rho^{(i)}(x + a^{-1}\tau))| < \overline{q},\end{aligned}$$

and

$$\begin{aligned}\underline{\rho} < \tfrac{1}{2}(\rho_0^{(i)}(x - a^{-1}\tau) + \rho_0^{(i)}(2x_R^{(i)} - x - a^{-1}\tau) + \tfrac{1}{a}(d_j(\tau - a(x_R^{(i)} - x)) - q^{(i)}) < \overline{\rho},\\ |d_j(\tau - a(x_R^{(i)} - x)) + \tfrac{a}{2}(\rho^{(i)}(x - a^{-1}\tau) - \rho^{(i)}(2x_R^{(i)} - x - a^{-1}\tau))| < \overline{q},\end{aligned}$$

respectively.
Finally, if the steady densities in every pipeline is strictly larger than the lower bound $\underline{\rho}$, the initial conditions are Lipschitz continuous. Thus, the values of the transformed variables considered in Assumption (iv) vary continuously. Since the values of the transformed variables emanated from junction j depend continuously on the latter ones, a small neighborhood where Assumption (iv) holds exists by continuity arguments.

We note that, as it is obtained by a worst case scenario, the terminal time T is only a lower bound for the time, up to which solutions of (2) are guaranteed to exist. In all considered examples, the state of the system at time T still satisfies the assumptions of Proposition 4 and can be used as new initial conditions, providing a larger terminal time for all λ satisfying (8). However, this bootstrapping can not be always be applied.

REMARK 2. *Minor modifications of the results in [10] allow to establish BV-regularity of solutions to (2) provided the initial and boundary data as well as the friction coefficient are functions of bounded variation.*

In case of a single pipe we can establish higher regularity of the broad solutions. Provided, the friction coefficient λ is continuously differentiable with bounded derivative, the initial and boundary conditions are differentiable and suitably connected, methods from [1] can be applied to bounded domains and yield classical solutions of the problem.

For the subsequent development, let $\mathcal{S} = \mathcal{S}(\lambda)$ denote the solution operator of the underlying system (2), (IC) along with the boundary conditions (BC) for a given friction coefficient $\lambda \in L^1(\Omega)$, where (IC) might depend on λ.

3.3. Sensitivity Results for the Solution Operator. The results in this section are obtained for single pipes defined on $\Omega = (x_L, x_R)$. By linearity of the coupling condition, they can be directly extended to passive networks.

PROPOSITION 5. *Let $\lambda \in L^p(\Omega)$ with $p \in [1, \infty]$ satisfy (8). Moreover, let the initial conditions (IC) depend Lipschitz continuously on λ with respect to the $\|\cdot\|_{L^1(\Omega)}$ norm. Then the solution operator*

$$\mathcal{S} : L^p(\Omega) \to \mathbf{L}^\infty(\mathcal{Q})$$

is Lipschitz continuous for any $p \in [1, \infty]$.

Proof. Without loss of generality we assume $T \leq \overline{T}/2$. As already shown, $\mathcal{T}$, mapping $(X, \|\cdot\|_*)$ onto itself, defines a contraction on a subset of X defined by the pointwise bounds (14) - (16). According to (18), the contraction rate is $1/2$ for any λ satisfying (8). Parametrizing $\mathcal{T}$ by λ, for y^λ denoting the unique fixed point we obtain

$$\|y^{\lambda_1} - y^{\lambda_2}\|_* = \|\mathcal{T}_{\lambda_1}(y^{\lambda_1}) - \mathcal{T}_{\lambda_2}(y^{\lambda_2})\|_* \leq \|\mathcal{T}_{\lambda_1}(y^{\lambda_1}) - \mathcal{T}_{\lambda_2}(y^{\lambda_1})\|_* + \|\mathcal{T}_{\lambda_2}(y^{\lambda_1}) - \mathcal{T}_{\lambda_2}(y^{\lambda_2})\|_*$$

and the upper bound on the contraction rate of $\mathcal{T}_{\lambda_2}$ provides

$$\|y^{\lambda_1} - y^{\lambda_2}\|_* \leq 2\|\mathcal{T}_{\lambda_1}(y^{\lambda_1}) - \mathcal{T}_{\lambda_2}(y^{\lambda_1})\|_*.$$

By the definition of $\mathcal{T}_{\lambda_i}$ we further obtain

$$
\begin{aligned}
&(|(T_{\lambda_1})_i(y^{\lambda_1}) - (\mathcal{T}_{\lambda_2})_i(y^{\lambda_1})|)[\tau, x] \\
&\leq |c_i(y_0(\lambda_1) - y_0(\lambda_2))[\gamma_i(0;\tau,x)]| + (2ac_a)^{-1} \int_0^\tau \left| (\lambda_1 - \lambda_2)[\gamma_i(t;\tau,x)] \left(\frac{q^{\lambda_1}|q^{\lambda_1}|}{\rho^{\lambda_1}} \right) [t, \gamma_i(t;\tau,x)] \right| dt \\
&\leq L_\lambda \|\lambda_1 - \lambda_2\|_{L^1(\Omega)} \leq L_\lambda \|\lambda_1 - \lambda_2\|_{L^p(\Omega)}
\end{aligned}
$$

where $L_\lambda > 0$ depends on (14) - (16) and the Lipschitz constant for the initial data. Since this estimate is independent of the position (τ, x), it holds for the essential supremum. Finally we use $e^{-2CT} \leq e^{-2Ct} \leq e^0 = 1$, valid for all $t \geq 0$, and the matrix norm of L, induced by the $|\cdot|_\infty$-norm to find

$$
\|y^{\lambda_1} - y^{\lambda_2}\|_{\mathbf{L}^\infty(\mathcal{Q})} \leq 2L_\lambda |L|_\infty e^{2CT} \|\lambda_1 - \lambda_2\|_{L^p(\Omega)},
$$

ending the proof. ∎

Next we demonstrate that the trace evaluation of broad solutions at entry- or exit nodes of the network is Lipschitz continuous as well.

PROPOSITION 6. *Let $\{x_E\}$ denote an entry- or exit node of the network. Under the assumptions of Proposition 5, the trace evaluation of the density is Lipschitz continuous with respect to the friction parameter, i.e.,*

$$
\|\rho^{\lambda_1}(t, x_E) - \rho^{\lambda_2}(t, x_E)\|_{L^p(0,T)} \leq L \|\lambda_1 - \lambda_2\|_{L^q(\Omega)}
$$

for $p, q \in [1, \infty]$ and some $L_\not{\partial} 0$.

Proof. Without loss of generality we assume $T \leq \overline{T}/2$. By the structure of the differential operator, exactly one characteristic i approaches the corresponding lateral boundary. For a fixed $\tau \in (0, T)$ we obtain

$$
\begin{aligned}
&|(\mathcal{T}_i(y^{\lambda_1}) - \mathcal{T}_i(y^{\lambda_2}))[\tau, x_E]| \leq |(\mathcal{T}_i(y^{\lambda_1}) - \mathcal{T}_i(y^{\lambda_2}))[0, s_i(0;\tau,x_E)]| + \\
&\hat{L} \int_0^\tau |(\lambda_1 - \lambda_2)[s_i(t;\tau,x_E)]| dt + \overline{\lambda} \tilde{L} \int_0^\tau |(y^{\lambda_1} - y^{\lambda_2})[t, s_i(t;\tau,x_E)]|_{l_\infty} dt
\end{aligned}
$$

with constants $\tilde{L}, \hat{L}$ depending on (14) to (16). By assumption, $|(\mathcal{T}_i(y^{\lambda_1}) - \mathcal{T}_i(y^{\lambda_1}))[0, s_i(0;\tau,x_E)]|$ depends Lipschitz continuously on λ and, applying Proposition 5, we find some $L_\rho > 0$ such that

$$
|(\mathcal{T}_i(y^{\lambda_1}) - \mathcal{T}_i(y^{\lambda_2}))[\tau, x_E]| \leq L_\rho \|\lambda_1 - \lambda_2\|_{L^1(\Omega)}
$$

is satisfied for almost every $\tau \in (0, T)$ and thus for $\|\mathcal{T}_1(y^{\lambda_1}) - \mathcal{T}_1(y^{\lambda_2})[t, x_E]\|_{L^\infty(0,T)}$. Since $T < \infty$, the claimed estimate follows from the continuous embedding $L^q(0,T) \hookrightarrow L^p(0,T)$ for $p, q \in [1, \infty], p \leq q$. ∎

Let the initial conditions be differentiable with respect to λ. For establishing differentiability of $\mathcal{S}$, we consider the following linear system, which is based on $(\rho, q) = \mathcal{S}(\lambda)$ with λ satisfying (8):

$$
\begin{aligned}
\mu_t + \nu_x &= 0, \\
\nu_t + a^2 \mu_x &= -2\lambda \frac{|q|}{\rho} \nu + \lambda \frac{q|q|}{\rho^2} \mu - h \frac{q|q|}{\rho}.
\end{aligned} \tag{19}
$$

Moreover, along with a perturbation direction h for λ, we consider the initial conditions

$$
\mu(0, \cdot) = \rho_0'(\lambda)[h], \quad \nu(0, \cdot) = q_0'(\lambda)[h] \text{ for } x \in \Omega, \tag{20}
$$

the coupling conditions (4) and (5) for ν and μ, respectively, in case of a network and the boundary condition

$$\nu(t, x_E) = 0 \text{ for } t \in (t, T) \tag{21}$$

for all entry- or exit nodes x_E. Since the problem is linear and (ρ, q) satisfies (14)-(16), the existence of a broad solution follows directly from the arguments given in [10] or, in case of a network, as discussed above. Concerning differential sensitivity of (ρ, q) we have the following assertion.

PROPOSITION 7. *The solution operator $\mathcal{S}$ is directional differentiable and the derivative at λ in direction h, i.e. $v = \mathcal{S}'(\lambda)[h]$, is characterized as the broad solution of (19) with initial and boundary conditions (20)-(21).*

Proof. Without loss of generality we assume $T \leq \overline{T}$ and consider $\tilde{y} = \mathcal{S}(\lambda + h)$ and $y = \mathcal{S}(\lambda)$ as well as $(\mu, \nu) = v$, the solution to (19)-(21). Studying $\mathcal{S}(\lambda+h) - \mathcal{S}(\lambda) - v$, the associated system satisfied by $(r, k) = (\tilde{\rho} - \rho - \mu, \tilde{q} - q - \nu)$ yields

$$\begin{aligned}
r_t + k_x &= 0,\\
k_t + a^2 r_x &= -(\lambda + h)\frac{\tilde{q}|\tilde{q}|}{\tilde{\rho}} + \lambda\frac{q|q|}{\rho} + 2\lambda\frac{|q|}{\rho}\nu - \lambda\frac{q|q|}{\rho^2}\mu + h\frac{q|q|}{\rho}\\
&= \lambda\left(-\frac{\tilde{q}|\tilde{q}|}{\tilde{\rho}} + \frac{q|q|}{\rho} + 2\frac{|q|}{\rho}\nu - \frac{q|q|}{\rho^2}\mu\right) + h\left(\frac{q|q|}{\rho} - \frac{\tilde{q}|\tilde{q}|}{\tilde{\rho}}\right)\\
&= \lambda\int_0^1 2\left(\frac{|\tilde{q} + l(q-\tilde{q})|}{\tilde{\rho} + l(\rho - \tilde{\rho})} - \frac{|q|}{\rho}\right)(q - \tilde{q})dl\\
&\quad + \lambda\int_0^1 \left(\frac{q|q|}{\rho^2} - \frac{\tilde{q} + l(q-\tilde{q})|\tilde{q} + l(q-\tilde{q})|}{(\tilde{\rho} + l(\rho - \tilde{\rho}))^2}\right)(\rho - \tilde{\rho})dl\\
&\quad - 2\lambda\frac{|q|}{\rho}k + \lambda\frac{q|q|}{\rho^2}r + \left(\frac{q|q|}{\rho} - \frac{\tilde{q}|\tilde{q}|}{\tilde{\rho}}\right)h\\
&=: f'(\tilde{y}, y, h; r, k)
\end{aligned} \tag{22}$$

with homogeneous boundary conditions for k at x_E, $r_0 = \rho_0(\lambda + h) - \rho_0(\lambda) - \rho_0'(\lambda)[h]$ and $k_0 = q_0(\lambda+h) - q_0(\lambda) - q_0'(\lambda)[h]$ and coupling conditions (4)-(5) for k and r, respectively. Further, as (r, k) can be expressed as the difference of broad solutions, it is a broad solution as well. In order to establish $\|(r, k)\|_{\mathbf{L}^\infty(\mathcal{Q})} = o(\|h\|_{L^1(\Omega)})$ with $o(t)/t \to 0$ as $t \to 0$, we consider the representation of broad solutions along integral curves. According to the structure of the source term of (22) and considering the structure of L^{-1} on page 3, we find $c_1 \cdot (0, f'(y))^\top = -c_2 \cdot (0, f'(y))^\top$. By homogeneous boundary conditions for ν and $\tilde{q}(\tau, x_E) = q(\tau, x_E)$, we find $k(\tau, x_E) = 0$, implying

$$\mathcal{T}_1(r, k)[\tau, x_E] = c_a^{-1}\left(\frac{1}{2}r - \frac{1}{2a}k\right)[\tau, x_E] = c_a^{-1}\left(\frac{1}{2}r + \frac{1}{2a}k\right)[\tau, x_E] = \mathcal{T}_2(r, k)[\tau, x_E].$$

As a consequence, the following estimate holds for all points $(\tau, x) \in \mathcal{Q}$ and $i = 1, 2$ including those, where the curves $\gamma_i(\cdot; \tau, x)$ (c.f., page 5) are mirrored at the boundaries x_E but not interact with internal nodes:

$$\begin{aligned}
&|\mathcal{T}_i(r, k)[\tau, x]|\\
&\leq c_i(y_0(\lambda + h) - y_0(\lambda) - y_0'(\lambda)[h]) + (2ac_a)^{-1}\int_0^\tau |f'(\tilde{\rho}, \tilde{q}, \rho, q, h; r, k)[t, \gamma_i(t; \tau, x)]|dt.
\end{aligned} \tag{23}$$

Next we analyze $|f'(\tilde{\rho}, \tilde{q}, \rho, q, h; r, k)[t, \gamma_2(t; \tau, x)]|$ term-wise. By (14)-(16), the original source term is Lipschitz continuous with respect to the state y. Moreover, the solution operator $\mathcal{S}$ is Lipschitz

continuous with respect to the friction coefficient λ providing

$$|h(\gamma_1(t;\tau,x))\left(\frac{q|q|}{\rho}-\frac{\tilde{q}|\tilde{q}|}{\tilde{\rho}}\right)[t,\gamma_1(t;\tau,x)]|\leq C\|h\|^2_{L^1(\Omega)} \text{ for all } (\tau,x)\in\mathcal{Q}$$

and some C¿0. For the terms with $0\leq l\leq 1$, we find

$$\left|\left(\frac{|\tilde{q}+l(q-\tilde{q})|}{\tilde{\rho}+l(\rho-\tilde{\rho})}-\frac{|q|}{\rho}\right)\right|\leq C\|\tilde{y}-y\|_{\mathbf{L}^\infty(\mathcal{Q})},$$
$$\left|\left(\frac{q|q|}{\rho^2}-\frac{(\tilde{q}+l(q-\tilde{q}))|\tilde{q}+l(q-\tilde{q})|}{(\tilde{\rho}+l(\rho-\tilde{\rho}))^2}\right)\right|\leq C\|\tilde{y}-y\|_{\mathbf{L}^\infty(\mathcal{Q})}.$$

for some $C>0$. Thus, the corresponding terms in f' can be estimated pointwise at (τ,x) by $C\|h\|^2_{L^1(\Omega)}$ with some suitably large $C>0$, again employing the Lipschitz continuity of $\mathcal{S}$. In case of $\gamma_i(t;\tau,x)$ interacting with an internal node x_I and $x\in(x_L^{(j)},x_R^{(j)})$, $\mathcal{T}_i^{(j)}(\underline{t}_i,x_I)$ is given as a linear combination of the transformed variables approaching x_I from all adjacent pipelines since the linear systems defining the original states have regular system matrices. Thus, we have weights $\hat{c}^I$ and

$$|\mathcal{T}_i^{(j)}(\underline{t}_i(\tau,x),x_I)|\leq\sum_{l\in n_L^I\cup n_R^I}|\hat{c}_l^I||\mathcal{T}_{\tilde{i}}^{(l)}(\underline{t}_i(\tau,x),x_I)|.$$

As before, the arguments for estimating (23) can be applied to the right-hand side. Further, since the initial condition is assumed to be sufficiently smooth we find

$$|\mathcal{T}_i(r,k)[\tau,x]|\leq C\|h\|^2_{L^p(\Omega)}+\tilde{C}\int_0^\tau|\mathcal{T}(r,k)|_\infty[t,\gamma_i(t;\tau,x)]dt$$

for $i=1,2$, $\tilde{C}>0$ sufficiently large and all $x\in\Omega$ and thus for $|\mathcal{T}(r,k)|_\infty[\tau,x]$. Here, $\tilde{C}$ depends on (14)-(16), and on the constants C above. Applying Gronwall's inequality to $u(t)=\operatorname{ess-sup}_{x\in\Omega}|\mathcal{T}(r,k)[t,\cdot]|_{l^\infty}$, we establish $u(\tau)\leq c(T)\|h\|^2_{L^1(\Omega)}$ for all $\tau\in[0,T]$. A suitable matrix norm of L finally provides $\|(r,k)\|_{\mathbf{L}^\infty(\mathcal{Q})}=o(\|h\|_{L^1(\Omega)})$ as $\|h\|_{L^1(\Omega)}\to 0$. ∎

Similar to Proposition 5, one can establish uniform Lipschitz continuity of the directional derivatives $\mathcal{S}'(\lambda)[h]$ with respect to λ. In addition, $\mathcal{S}'(\lambda)[h]$ is linear in h and consequently, $\mathcal{S}$ is Frechét differentiable. As in Proposition 6, this result can be extended to trace evaluations of ρ at the lateral boundary.

The section closes with a discussion of second-order differentiability. We point out that this result can be established only under a very restrictive condition.

PROPOSITION 8. *Let the volume flow have a constant direction along the entire network for all times $t\in(0,T)$. Moreover, let the initial conditions depend smoothly on λ. Then the solution operator is twice differentiable and $S''(\lambda)[h,\delta]$, for perturbation directions $h,\delta\in L^1(\Omega)$, is given as broad solution (s,p) of the system*

$$\begin{aligned}
s_t+p_x&=0,\\
p_t+a^2s_x&=-2\lambda\frac{|q|}{\rho}p+\lambda\frac{q|q|}{\rho^2}s-\delta\left(2\frac{|q|}{\rho}\nu_h-\frac{q|q|}{\rho^2}\mu_h\right)-h\left(2\frac{|q|}{\rho}\nu_\delta-\frac{q|q|}{\rho^2}\mu_\delta\right)\\
&\quad-2\lambda\frac{1}{\rho}\nu_\delta\mu_h-2\lambda\frac{q|q|}{\rho^3}\mu_\delta\mu_h+2\lambda\frac{|q|}{\rho^2}\mu_\delta\nu_h+2\lambda\frac{|q|}{\rho^2}\mu_h\nu_\delta,
\end{aligned}$$

with homogeneous boundary conditions at entry- and exit nodes for p, coupling conditions (4)-(5) for p and s and initial conditions

$$s(0,\cdot)=\rho_0''(\lambda)[h,\delta],\quad p(0,\cdot)=q_0''(\lambda)[h,\delta].$$

Proof. The proof is analogous to the one for establishing differentiability. A careful analysis of the remainder term of the associated expansion of $\mathcal{S}$ and properties of the involved states and their first-order derivatives in certain directions as well as the application of Gronwall's inequality provide an estimate for the remainder term at the order of $o(\|\delta\|_{L^1})$ as $\|\delta\|_{L^1(\Omega)} \to 0$. Here, δ denotes the corresponding perturbation.

To obtain the estimates as in the proof of lower order regularity, it is important, that the volume flow does not change its sign along the pipes since otherwise, the absolute value, present in the sensitivity equations, can not be handled as before. ∎

Note that the required constant direction of the volume flow translates into further conditions on initial and boundary conditions as well as on T. We emphasize that the assumptions of Proposition 8 were met in all numerical examples of Section 5.

4. The Identification Problem for the Friction Coefficient. After analyzing the underlying state system, we now focus on the identification problem for the friction coefficient as a distributed quantity within a single pipe defined on $\Omega = (x_L, x_R)$, based on measurements of the pressure at at the boundaries of the pipe. The corresponding output-least-squares formulation reads

$$(P)\qquad \begin{aligned} \text{minimize}\quad & \frac{1}{2}\|\rho(\cdot,x_L)-\rho_L^d(\cdot)\|^2_{L^2(0,T)} + \frac{1}{2}\|\rho(\cdot,x_R)-\rho_R^d(\cdot)\|^2_{L^2(0,T)} + \alpha\mathcal{R}(\lambda) =: \mathcal{J}(\lambda)\\ \text{over}\quad & y \in \mathbf{L}^\infty(\mathcal{Q}), \lambda \in L^1(\Omega), \lambda \in \mathcal{D}(\mathcal{R})\\ \text{subject to}\quad & \|\lambda\|_{L^1(\Omega)} \le \overline{\lambda},\\ & y = \mathcal{S}(\lambda). \end{aligned}$$

The functions $\rho_L^d(\cdot), \rho_R^d(\cdot) \in L^2(0,T)$ represent the, possibly perturbed, measured data at the left and right end of the pipe over time. Moreover, the solution operator might include initial conditions that depend smoothly on λ. Finally, $\mathcal{R}$ denotes a suitable regularization term based on a priori assumptions on the structure of the friction parameter. Let $\mathcal{D}(\mathcal{R}) \subset L^1(\Omega)$ denote the domain space of $\mathcal{R}$.

PROPOSITION 9. *Let the domain space of the regularization term $\mathcal{D}(\mathcal{R})$ embed compactly into $L^p(\Omega)$ for some $p \in [1,\infty]$. Then (P) admits a solution.*

Proof. By assumption, the domain of the regularizer embeds compactly into $L^p(\Omega)$ and Proposition 5 guarantees continuity of $\mathcal{S}$ with respect to this space. Then the result follows from an application of the direct method from the calculus of variations. ∎

The assumption of $\mathcal{D}(\mathcal{R})$ compactly embedding into $L^1(\Omega)$, is met, e.g., by choosing $\mathcal{R} = |\cdot|_{TV}$ with $|\cdot|_{TV}$ the total variation seminorm.

5. Numerical Experiment.

Identification of pipelinewise constant friction coefficients in a network. The network under consideration is depicted in Figure 1 and can be seen as supply network for, e.g., gas power plants located at the exit nodes 'Exit 1' and 'Exit 2' that require constant supply while the inflow in the network at the entry node 'In' varies over time. At the respective nodes, boundary conditions for q are fixed as the functions provided in Figure 1. The initial conditions are considered to be steady states according to (9) with $q_0 = [300, 180, 120]$ with pipes being numbered counter-clockwise, beginning with the one at the in-node and for $\rho_0(x_{In}) = 52.3$. The values $l^{(i)} = x_R^{(i)} - x_L^{(i)}$ denote the length of the pipes $1 \le i \le 3$. The underlying partial differential equation fails to admit a classical solution and, as outlined above, the gradient is generated according to the sensitivity system (19) along with the corresponding initial and boundary conditions as discussed in Example 2. If time-discrete measurements of density at 'Exit 1' and 'Exit 2' are considered, the identification problem of pipeline wise constant friction coefficients becomes a finite dimensional problem. In this case, the identification problem in its output-least-squares

formulation is given as

$$
\begin{aligned}
\text{minimize}\ & \tfrac{1}{2}\Big(\sum_{i=0}^{20}(\rho(10\cdot i, x_{E_1}) - \rho^d_{E_1}(10\cdot i))^2 + (\rho(10\cdot i, x_{E_2}) - \rho^d_{E_2}(10\cdot i))^2\Big) + \tfrac{\alpha}{2}\|\lambda - \lambda_M\|^2_{l^2} \\
& =: \mathcal{J}(\lambda) \\
\text{subject to}\ & (\rho^{(i)}, q^{(i)}) = \mathcal{S}(\lambda^{(i)}) \text{ on } (0,T)\times(x_L^{(i)}, x_R^{(i)}), \\
& (\rho^{(i)}(0,x), q^{(i)}(0,x)) \text{ solves (9) with given } q_0^{(i)} \text{ for } \lambda^{(i)}, \\
& \rho(t, x_R^{(1)}) = \rho(t, x_L^{(2)}) = \rho_L^{(3)},\ \ q^{(1)}(t, x_R^{(1)}) = q^{(2)}(t, x_L^{(2)}) + q^{(3)}(t, x_L^{(3)}), \\
& q^{(1)}(t, x_L^{(1)}) = q^d_{In}(t), q^{(2)}(t, x_R^{(2)}) = q^d_{Exit_1}(t), q^{(3)}(t, x_R^{(3)}) = q^d_{Exit_2}(t), \\
& \rho^{(1)}(t, x_L^{(1)}) = 52.3, \\
& 10^{-9} \le \lambda^{(i)} \le \overline{\lambda},
\end{aligned}
$$

and admits a solution by standard arguments of variational analysis as utilized in Proposition 9.

In the finite dimensional case, the integral bound on λ translates into a pipeline wise upper bound and we used $\overline{\lambda}^{(i)} = 2$. In addition, we assume strict positivity of λ, realized by a component-wise lower bound of 10^{-9} providing, together with the upper bound, box constraints. the terminal time is given by $T = 200$ and the regularization weight in the objective is chosen as $\alpha = 10$ with $\mathcal{R}(\cdot) = \frac{1}{2}|\cdot|^2_{l^2}$. The value $\lambda_M = 0.018172$ represents a-priori knowledge on the friction coefficient obtained from practitioners.

5.1. Algorithm. In order to solve the identification problem we employ a Trust-region method (see [2]) where the model of the function is based on a quasi-Newton approximation of the Hessian (see [17]), utilizing the BFGS-update and including a reset of the approximating matrix in case of the update direction failing the test for the curvature condition. The procedure is described in Algorithm 1.

Using second order derivatives is motivated by the considered initial conditions and Proposition 3 and Proposition 8 implying, that the solution operator is twice Fréchet differentiable. The constants for incrementing the Trust-region radius are chosen according to the suggestions in [2, Page 117]. The algorithm terminates, if norm of the gradient in iteration k satisfies

$$\|\nabla\mathcal{J}(\lambda^{(k)})\|_{\ell^2} \le \nu_{rel}\|\nabla\mathcal{J}(\lambda^{(0)})\|_{\ell^2} + \nu_{abs}$$

with $\nu_{abs} = \nu_{rel} = 10^{-7}$.

Next we discuss the Trust-region sub-problem (24). Again, the existence of solutions follows from standard arguments of variational analysis. The update strategy for the approximation of the Hessian ensures positive definiteness of H_k and thus, the solution of the now convex problem (24) is unique.

One easily checks, that the linear independent constraint qualification is satisfied if $10^{-9} < \overline{\lambda}$ holds. As a consequence, Lagrange multipliers $\psi_0 \in \mathbb{R}, \psi_1 \in \mathbb{R}^3, \psi_2 \in \mathbb{R}^3$, associated with the radius constraint, the component-wise lower and upper bound, respectively, exist. The optimality system that characterizes the solution x of (24) and the corresponding Lagrange multipliers, $(x, \psi_0, \psi_1, \psi_2)$, reads

$$
\begin{aligned}
\nabla\mathcal{J}(\lambda_k) + (H_k x)^\top - 2\psi_0 x + \psi_1 - \psi_2 &= 0, \\
\Delta_k^2 - \|x\|^2_{l^2} \ge 0, \psi_0 \ge 0, \psi_0(\Delta_k^2 - \|x\|^2_{l^2}) &= 0, \\
x + \lambda_k - 10^{-9} \ge 0, \psi_1 \ge 0, \psi_1(x + \lambda_k - 10^{-9}) &= 0, \\
\overline{\lambda} - \lambda_k - x \ge 0, \psi_2 \ge 0, \psi_2(\overline{\lambda} - \lambda_k - x) &= 0,
\end{aligned} \tag{25}
$$

where the last two lines are considered component-wise. Utilizing the nonlinear complementarity function

$$0 \le a, 0 \le b, ab = 0 \Leftrightarrow 0 = a - \max\{0, a - \nu_{SSN} b\},$$

Algorithm 1 Trust Region

Choose λ_0, compute $\mathcal{J}(\lambda_0), \nabla\mathcal{J}(\lambda_0)$.
Set $k = 0, \eta_1 = 0.01, \eta_2 = 0.9, \kappa_1 = 2, \kappa_2 = 0.75, \kappa_3 = 0.5, H_k = I, \Delta_k = 10^{-4}$.
while stopping criterion not satisfied **do**
  Define quadratic model $m_k(\lambda_k + s) = \mathcal{J}(\lambda_k) + < \nabla\mathcal{J}(\lambda_k), s > + < s, H_k s >$
  Solve trust-region sub-problem

$$\begin{aligned} &\text{minimize } m_k(\lambda_k + x) \\ &\quad \text{over } x \in \mathbb{R}^3 \\ &\text{subject to } \|x\|_{l^2}^2 \le \Delta_k^2, \\ &\qquad 10^{-9} - \lambda_k \le x \le \overline{\lambda} - \lambda_k \end{aligned} \tag{24}$$

  Compute $\mathcal{J}(\lambda_k + x)$ and define

$$\mathfrak{r}_k := \tfrac{\mathcal{J}(\lambda_k) - \mathcal{J}(\lambda_k + x)}{m_k(\lambda_k) - m_k(\lambda_k + x)}.$$

  Update the iterate according to

$$\lambda_{k+1} = \begin{cases} \lambda_k + x & \text{if } \mathfrak{r}_k \ge \eta_1 \\ \lambda_k & \text{else} \end{cases}.$$

  Update the Trust-region radius according to

$$\Delta_{k+1} = \begin{cases} \kappa_1 \Delta_k & \text{if } \mathfrak{r}_k \ge \eta_2 \\ \kappa_2 \Delta_k & \text{if } \mathfrak{r}_k \in [\eta_1, \eta_2) \\ \kappa_3 \Delta_k & \text{if } \mathfrak{r}_k < \eta_1 \end{cases}.$$

  Compute $y_k = \nabla J(\lambda_{k+1}) - \nabla J(\lambda_k)$, update the approximation of the Hessian according to

$$H_{k+1} = \begin{cases} I & \text{if } < x, y_k > \le 0 \\ H_k + \frac{<y_k, y_k>}{<x, y_k>} - \frac{<H_k x, H_k x>}{x, H_k x} & \text{if } < x, y_k > > 0 \text{ and } \mathfrak{r}_k \ge \eta_1 \\ H_k & \text{if } \mathfrak{r}_k < \eta_1 \end{cases}.$$

  Set $k := k + 1$
end while

(for information on NCP-functions, we refer to [22]), (25) can be rewritten as the nonsmooth system

$$\begin{aligned} \nabla\mathcal{J}(\lambda_k) + (H_k x)^\top - 2\psi_0 x + \psi_1 - \psi_2 &= 0, \\ \psi_0 - (\psi_0 - \nu_{SSN}(\Delta_k^2 - \|x\|_{l^2}^2))^+ &= 0, \\ \psi_1 - (\psi_1 - \nu_{SSN}(x + \lambda_k - 10^{-9}))^+ &= 0, \\ \psi_2 - (\psi_2 - \nu_{SSN}(\overline{\lambda} - \lambda_k - x))^+ &= 0, \end{aligned} \tag{26}$$

with $(\cdot)^+ = \max\{0, \cdot\}$. System (26) is solved by applying the semismooth Newton method as discussed in [19], initialized with 0 and utilizing an Armijo line search for globalization. The semismooth Newton method terminates if the Euclidean norm of the residual drops below 10^{-9}.

5.2. Discretization of the underlying PDE and sensitivity equation. For the numerical realization of a gradient based descent algorithm for solving the inverse problem we apply an explicit discretization scheme utilizing piecewise constant cell averages of the state functions in the forward and sensitivity problem, (2) and (19), respectively, on a uniform grid dividing pipes into N cells of width Δx, which are referred to as internal cells. Of course, alternative discretization

schemes for semilinear systems of hyperbolic balance laws in the context of gas transport like the ones in, e.g., [21, 24] are possible as well. The boundary and coupling conditions at entry- and exit nodes and junctions are realized by ghost cells, i.e. each pipe has a ghost cell on both ends as depicted in Figure 3. While, within the pipe, the successive sequence of iterates with respect to

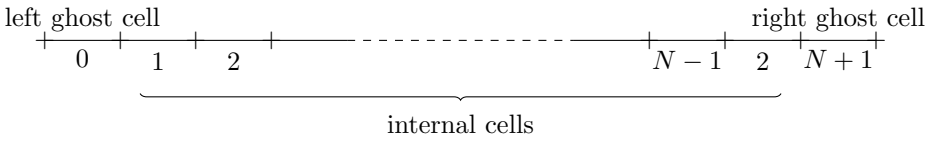

Fig. 3: Spatial discretization of a pipe whit ghost cells

time will be obtained by applying a total variation diminishing (TVD) discretization scheme combined with a Runge Kutta (RK) higher order time stepping (see [13]), the coupling and boundary conditions on the ghost cells have to be incorporated carefully. Before discussing the latter point, we provide a brief description of the numerical scheme utilized on the internal cells. Ignoring for a moment the source term we apply the modified Lax-Friedrichs scheme as used in [9, 23] and given in vector notation by

$$y_i^{n+1} = \tfrac{1}{2}(\gamma y_{i-1}^n - (2\gamma - 2)y_i^n + \gamma y_{i+1}^n) - \tfrac{c_{CFL}}{2} A(y_{i+1}^n - y_{i-1}^n), \tag{27}$$

with $c_{CFL} = a^{-1}$, providing N_T time steps. Here, $y_i^n = (\rho_i^n, q_i^n) \in \mathbb{R}^2$ for $1 \le n \le N_T$ and $1 \le i \le N$ denote the integral averages of density and volume flow in internal cell i and for time step n. For $\gamma = 1$, we obtain the original Lax-Friedrichs scheme that coincides, by linearity of the differential operator, also with the Engquist-Osher scheme as well.

Incorporation of the source term can be realized in several ways. On the one hand, one can apply splitting techniques like the first-order Godunov- or the second order Strang splitting or plain inclusion as in [23] for scalar balance laws. Note that, by the given source term, both approaches act merely on the second component of the state vector in each iteration of the time stepping. On the other hand, one can take into account the semilinear nature of the underlying system of partial differential equations and the definition of broad solutions. Consequently, one defines a numerical scheme similar to the particle method of [6] that is consistent with entropy solutions of scalar conservation laws and was used for semilinear systems of conservation laws in [10, 11]. Here, at time step n an explicit Euler method is utilized to approximate the solutions to (7) for each component of the transformed variables , i.e., for the first characteristic,

$$\mathcal{T}_1(y_{i-1}^{n+1}) = \mathcal{T}_1(y_i^n) + \tfrac{\Delta t}{c_a a} \lambda_i \tfrac{q_i^n |q_i^n|}{\rho_i^n},$$

and for $\mathcal{T}_2$, respectively. For equidistantly distributed particles with distance Δx, a time step $\Delta t = a^{-1}\Delta x$ and integral averages y_i^n and λ_i, the original state variables can be reconstructed according to (17), yielding the discretization scheme

$$\begin{aligned} \rho_i^{n+1} &= \tfrac{1}{2}(\rho_{i+1}^n + \rho_{i-1}^n) - \tfrac{c_{CFL}}{2}(q_{i+1}^n - q_{i-1}^n) - \tfrac{\Delta t}{2a}\left(\lambda_{i-1}\tfrac{q_{i-1}^n|q_{i-1}^n|}{\rho_{i-1}^n} - \lambda_{i+1}\tfrac{q_{i+1}^n|q_{i+1}^n|}{\rho_{i+1}^n}\right), \\ q_i^{n+1} &= \tfrac{1}{2}(q_{i+1}^n + q_{i-1}^n) - \tfrac{a^2 c_{CFL}}{2}(\rho_{i+1}^n - \rho_{i-1}^n) - \tfrac{\Delta t}{2}\left(\lambda_{i-1}\tfrac{q_{i-1}^n|q_{i-1}^n|}{\rho_{i-1}^n} + \lambda_{i+1}\tfrac{q_{i+1}^n|q_{i+1}^n|}{\rho_{i+1}^n}\right), \end{aligned} \tag{28}$$

for $i = 1, ..., N$, corresponding to the Lax-Friedrichs scheme.

The similarity of the particle method, mirroring the nature of broad solutions by integrating along characteristic lines, to a classical TVD discretization scheme suggests a procedure for obtaining the values of the state at the ghost cells by employing the concept of broad solutions in the following way. At entry- or exit-nodes of the network, the updated value for the state is obtained by evaluating the ingoing transformed variable and solving the linear systems defined by the matrices C_L or C_R respectively, i.e, to solve

$$C_L^{-1}\begin{pmatrix} \mathcal{T}_1(y_0^{n+1}) \\ d_0(t^{n+1}) \end{pmatrix} \text{ and } C_R^{-1}\begin{pmatrix} \mathcal{T}_2(y_{N+1}^{n+1}) \\ d_{N+1}(t^{n+1}) \end{pmatrix},$$

for boundary data d_0, d_{N+1} on the left and right ghost cell, respectively. Explicitly, this provides

$$\begin{aligned} \rho_{0/N+1}^{n+1} &= \rho_{1/N}^{n} \mp \tfrac{1}{a} q_{1/N}^{n} \pm \tfrac{1}{a} d_{0/N+1}(t^{n+1}) \pm \tfrac{\Delta t}{a} \lambda_{1/N} \frac{q_{1/N}^{n} |q_{1/N}^{n}|}{\rho_{1/N}^{n}}, \\ q_{0/N+1}^{n+1} &= d_{0/N+1}(t^{n+1}). \end{aligned} \tag{29}$$

At junctions, all ingoing transformed variables and the coupling conditions form linear systems that have to be solved for the values of the state variables on the corresponding ghost cells. For the example under consideration, the lienar system at the junction is given as (6).

Summarizing, we have established an algebraic expression that provides the updated state at all ghost cells g of the network, based on the current iterate and the boundary conditions at the next time step $d(t^{n+1})$, i.e., $(\rho_g^{n+1}, q_g^{n+1}) = f_g(\rho^n, q^n, \lambda, d(t^{n+1}))$.

Note that in case of implicit time stepping schemes as the IBox method ([3, 15]) this discussion is not necessary since coupling and boundary condition are considered directly in the nonlinear system that characterizes the next time step.

For the sake of comparison, Figure 4 depicts the trace evaluation of the pressure at Exit 1 in the setting of Example 5 below for different methods for handling the source term and several mesh widths. The results suggest that all methods converge but, by merely acting on the

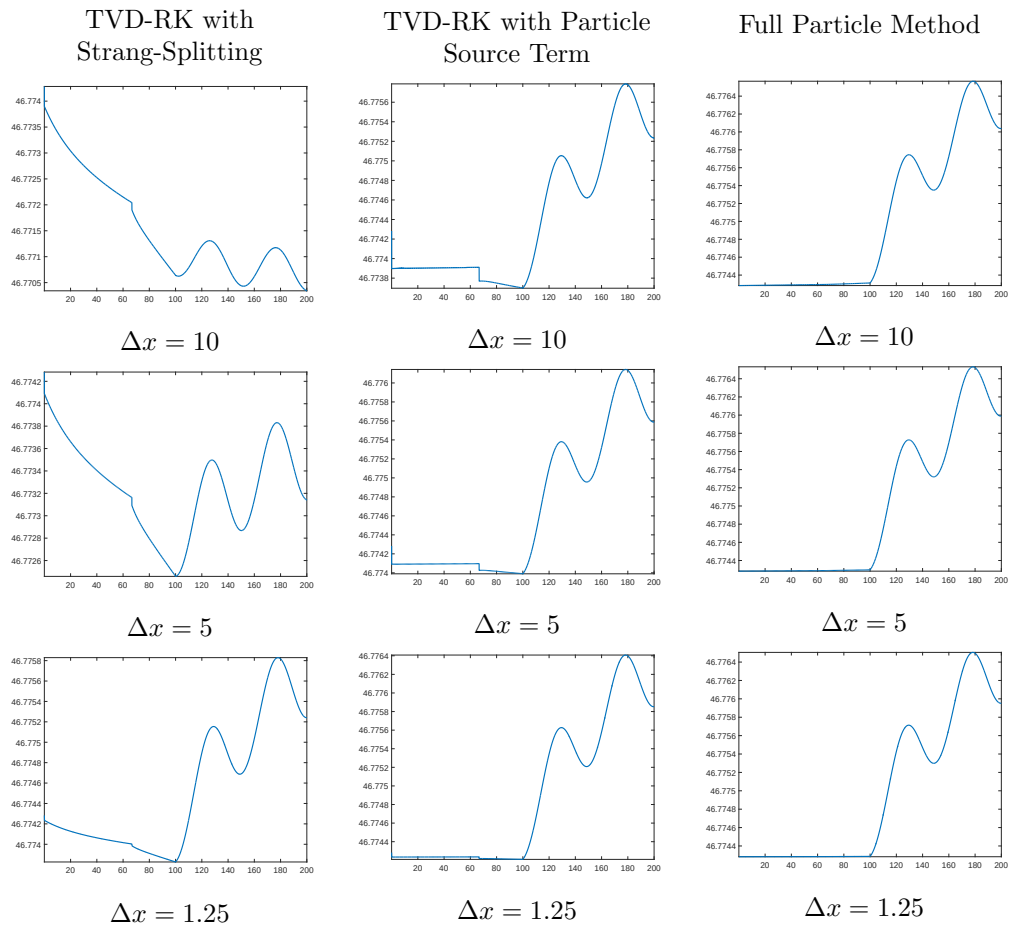

Fig. 4: trace evaluations of ρ for different discretization methods

second component of the state vector, the discretization method employing the Strang splitting is not satisfying as it gives qualitatively wrong solutions even on fine meshes. Note that the discontinuities exhibited in the first two columns of Figure 4 at the initial time and near $t \approx 70$

are based on the fact that integral averages of the stationary initial state and the values at the ghost cells do not provide a stationary state for the discrete problem. However, by refining the discretization, these effects vanish. The Lax-Friedrichs scheme with the source term handling inspired by the particle method behaves more stable. Hence, we utilize this procedure in what follows, i.e., we employ (28) under a further slight modification which, in componentwise form, reads

(30)
$$\begin{aligned}\rho_i^{n+1} &= \tfrac{1}{2}(\gamma\rho_{i+1}^n - (2\gamma-2)\rho_i^n + \gamma\rho_{i-1}^n) - \tfrac{c_{CFL}}{2}(q_{i+1}^n - q_{i-1}^n) - \tfrac{\Delta t}{2a}\lambda_i\left(\tfrac{q_{i-1}^n|q_{i-1}^n|}{\rho_{i-1}^n} - \tfrac{q_{i+1}^n|q_{i+1}^n|}{\rho_{i+1}^n}\right),\\ q_i^{n+1} &= \tfrac{1}{2}(\gamma q_{i+1}^n - (2\gamma-2)q_i^n + \gamma q_{i-1}^n) - \tfrac{a^2 c_{CFL}}{2}(\rho_{i+1}^n - \rho_{i-1}^n) - \tfrac{\Delta t}{2}\lambda_i\left(\tfrac{q_{i-1}^n|q_{i-1}^n|}{\rho_{i-1}^n} + \tfrac{q_{i+1}^n|q_{i+1}^n|}{\rho_{i+1}^n}\right).\end{aligned}$$

Note that (30) correspinds to an explicit Euler discretization of the ODE system

(31)
$$\begin{aligned}\dot\rho_i &= \tfrac{\gamma}{2\Delta t}(\rho_{i+1} - 2\rho_i + \rho_{i-1}) - \tfrac{c_{CFL}}{2\Delta t}(q_{i+1} - q_{i-1}) - \tfrac{1}{2a}\lambda_i\left(\tfrac{q_{i-1}|q_{i-1}|}{\rho_{i-1}} - \tfrac{q_{i+1}|q_{i+1}|}{\rho_{i+1}}\right) = f_{\rho_i},\\ \dot q_i &= \tfrac{\gamma}{2\Delta t}(q_{i+1} - 2q_i + q_{i-1}) - \tfrac{a^2 c_{CFL}}{2\Delta t}(\rho_{i+1} - \rho_{i-1}) - \tfrac{1}{2}\lambda_i\left(\tfrac{q_{i-1}|q_{i-1}|}{\rho_{i-1}} + \tfrac{q_{i+1}|q_{i+1}|}{\rho_{i+1}}\right) = f_{q_i},\end{aligned}$$

with associated initial conditions. in order to obtain a higher-order approximation of these ODE's with respect to time, we apply, similar to [9, 13] a Runge-Kutta time stepping method to (31), namely the second-order method of Heun and obtain the full discretization scheme

(32)
$$\begin{aligned}\bar\rho_i^n &= f_{\rho_i}(\rho^n, q^n, \lambda),\\ \bar q_i^n &= f_{q_i}(\rho^n, q^n, \lambda),\\ \rho_i^{n+1} &= \rho_i^n + \tfrac{\Delta t}{2}(f_{\rho_i}(\rho^n, q^n, \lambda) + f_{\rho_i}(\rho^n + \Delta t\bar\rho^n, q^n + \Delta t\bar q^n, \lambda)),\\ q_i^{n+1} &= q_i^n + \tfrac{\Delta t}{2}(f_{q_i}(\rho^n, q^n, \lambda) + f_{q_i}(\rho^n + \Delta t\bar\rho^n, q^n + \Delta t\bar q^n, \lambda)),\end{aligned}$$

on the interior cells while the ghost cells are updated according to

$$\begin{aligned}(\bar\rho_g^n, \bar q_g^n) &= \Delta t^{-1}(f_g(\rho^n, q^n, \lambda, d^{n+1}) - (\rho_g^n, q_g^n)),\\ (\rho_g^{n+1}, q_g^{n+1}) &= (\rho_g^n, q_g^n) + \tfrac{\Delta t}{2}((\bar\rho_g^n, \bar q_g^n) + \Delta t^{-1}(f_g(\bar\rho^n, \bar q^n, \lambda, d^{n+1}) - (\rho_g^n, q_g^n))).\end{aligned}$$

The latter has been chosen to obtain the correct boundary value for q_g^{n+1} while having the form of the Heun scheme.

Similar to [9, 13, 23], the sensitivity scheme for interior cells is obtained by linearizing (32). Let μ_i^n and ν_i^n denote the derivatives of p_i^n and q_i^n with respect to p_j^{n-1}, q_j^{n-1} and λ_j respectively and $v_i^n = (\mu_i^n, \nu_i^n)$ the state , providing

(33)
$$\begin{aligned}\bar\mu_i^n =& \tfrac{\gamma}{2\Delta t}(\mu_{i+1}^n - 2\mu_i^n + \mu_{i-1}^n) - \tfrac{c_{CFL}}{2\Delta t}(\nu_{i+1}^n - \nu_{i-1}^n) - \tfrac{1}{2a}l_i\left(\tfrac{q_{i-1}^n|q_{i-1}^n|}{\rho_{i-1}^n} - \tfrac{q_{i+1}^n|q_{i+1}^n|}{\rho_{i+1}^n}\right)\\ &. + \tfrac{1}{2a}\lambda_i\left(\tfrac{q_{i-1}^n|q_{i-1}^n|}{(\rho_{i-1}^n)^2}\mu_{i-1}^n - \tfrac{q_{i+1}^n|q_{i+1}^n|}{(\rho_{i+1}^n)^2}\mu_{i+1}^n\right) - \tfrac{1}{a}\lambda_i\left(\tfrac{|q_{i-1}^n|}{\rho_{i-1}^n}\nu_{i-1}^n - \tfrac{|q_{i+1}^n|}{\rho_{i+1}^n}\nu_{i+1}^n\right) = f_{\mu_i},\\ \bar\nu_i^n =& \tfrac{\gamma}{2\Delta t}(\nu_{i+1}^n - 2\nu_i^n + \nu_{i-1}^n) - a^2\tfrac{c_{CFL}}{2\Delta t}(\mu_{i+1}^n - \mu_{i-1}^n) - \tfrac{1}{2}l_i\left(\tfrac{q_{i-1}^n|q_{i-1}^n|}{\rho_{i-1}^n} + \tfrac{q_{i+1}^n|q_{i+1}^n|}{\rho_{i+1}^n}\right)\\ &+ \tfrac{1}{2}\lambda_i\left(\tfrac{q_{i-1}^n|q_{i-1}^n|}{(\rho_{i-1}^n)^2}\mu_{i-1}^n + \tfrac{q_{i+1}^n|q_{i+1}^n|}{(\rho_{i+1}^n)^2}\mu_{i+1}^n\right) - \lambda_i\left(\tfrac{|q_{i-1}^n|}{\rho_{i-1}^n}\nu_{i-1}^n + \tfrac{|q_{i+1}^n|}{\rho_{i+1}^n}\nu_{i+1}^n\right) = f_{\nu_i},\\ \mu_i^{n+1} =& \mu_i^n + \tfrac{\Delta t}{2}\left(\bar\mu_i^n + f_{\mu_i}(y^n + \Delta t\bar y^n, v^n + \Delta t\bar v, \lambda)\right),\\ \nu_i^{n+1} =& \nu_i^n + \tfrac{\Delta t}{2}\left(\bar\nu_i^n + f_{\nu_i}(y^n + \Delta t\bar y^n, v^n + \Delta t\bar v, \lambda)\right),\end{aligned}$$

with initial conditions

$$\mu_i^0 = \tfrac{d\rho_i^0}{d\lambda_i}, \quad \nu_i^0 = \tfrac{dq_i^0}{d\lambda_i}, \tag{34}$$

and variations of the friction coefficient in the internal cell i, l_i. Updating the values on ghost cells is based on a linearization of the ordinary differential equations describing the flow into these

nodes and solving the resulting linear systems. For the example (29) of entry- and exit nodes we obtain

$$
\begin{aligned}
\mu^{n+1}_{0/N+1} =& \mu^n_{1/N} \mp \tfrac{1}{a}\nu^n_{1/N} \pm \tfrac{\Delta t}{a} l_{1/N} \tfrac{q^n_{1/N}|q^n_{1/N}|}{\rho^n_{1/N}} \\
& \pm \tfrac{2\Delta t}{a}\lambda_{1/N}\tfrac{|q^n_{1/N}|}{\rho^n_{1/N}}\nu^n_{1/N} \mp \tfrac{\Delta t}{a}\lambda_{1/N}\tfrac{q^n_{1/N}|q^n_{1/N}|}{(\rho^n_{1/N})^2}\mu^n_{1/N}, \\
\nu^{n+1}_{0/N+1} =& 0.
\end{aligned} \tag{35}
$$

Combining these linearized boundary conditions in the function $f'_g(y, v, \lambda)$, the update for the ghost cells g is given by

$$
\begin{aligned}
(\bar\mu^n_g, \bar\nu^n_g) &= \Delta t^{-1}(f'_g(y^n, v^n, \lambda) - (\mu^n_g, \nu^n_g)), \\
(\mu^{n+1}_g, \nu^{n+1}_g) &= (\mu^n_g, \nu^n_g) + \tfrac{\Delta t}{2}((\bar\mu^n_g, \bar\nu^n_g) + \Delta t^{-1}(f'_g(y^n + \Delta t\bar y^n, v^n + \Delta t\bar v^n, \lambda) - (\mu^n_g, \nu^n_g))).
\end{aligned}
$$

5.3. Example. In all computations presented next, the speed of sound is $a = 300ms^{-1}$ and the density ρ is in the range of $50kgm^{-3}$ corresponding to a pressure $p = a^2\rho$ around 45 bar.

Algorithm 1 is initialized by $\lambda^0 = (0.03, 0.03, 0.03)^\top$, again for pipes being numbered counter-clockwise, and the initial TR-radius is $\Delta_0 = 5 \cdot 10^{-4}$ and the mesh width for the numerical approximation of solutions to the state and sensitivity system is $\Delta x = 1.25$.

For testing purposes, we generated artificial data for the density at the exit nodes, assuming a friction coefficient of $\lambda^O = (0.018172, 0.018195, 0018145)^\top$ which reflects possible values for the friction of natural gas at a Reynolds number of 10^5. The data were generated by the particle method on a fine mesh and can be found in Figure 5 and 6. To we added Gaussian random noise with mean zero and a variance of 10^{-3} at measurement times. The variance has been chosen that small as the fluctuation of the density at the exit-nodes are already in the order of 10^{-3}. Thus, for larger variance the random perturbations dominate the desired state.

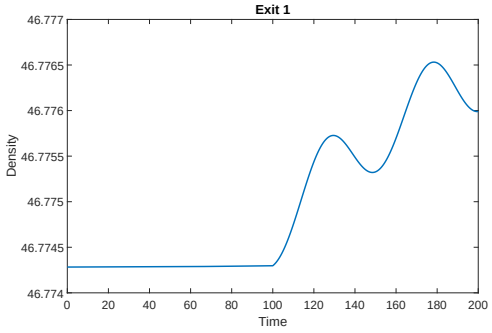

Fig. 5: Density for the original λ at Exit 1

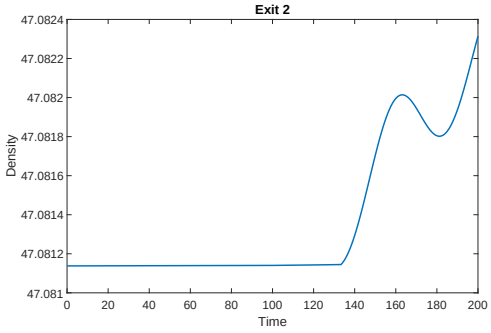

Fig. 6: Density for the original λ at Exit 2

Our reconstruction is

$$\lambda^* = (0.018346, 0.017952, 0.017785)^\top.$$

In Figure 7 we provide the difference of the iterates λ^i to the values λ^O over the iterations. Finally, the norm the gradient is shown in Figure 8. Note that the iterations 32 - 64 are null-steps in the sense that no update is performed but the radius of the trusted region is decreased. Fast convergence in the last iterations of the algorithm could be observed in any test run with different realizations of the random noise. Note that while the first component of λ^* exceeds the original value, the other components undershoot their respective values. This is a consequence of the coupling conditions since, given a larger friction coefficient in the first pipeline, the density decreases not enough which has to be compensated in the following pipelines by a larger friction coefficient to still approximate the measurements, and vice versa.

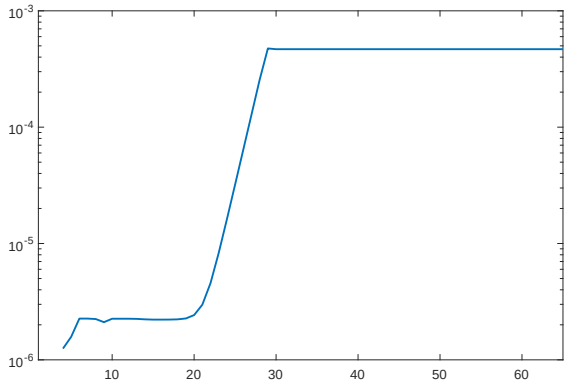

Fig. 7: Eucledian Norm $|\lambda^i - \lambda^O|$

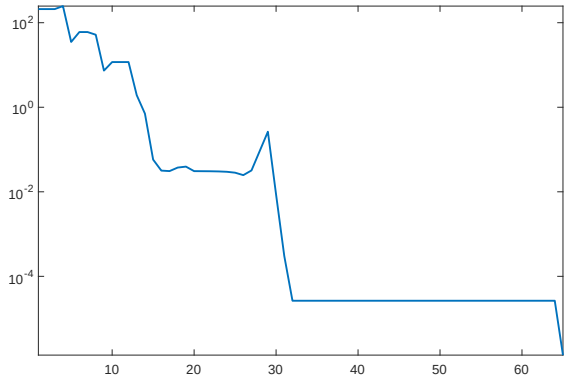

Fig. 8: Norm of the gradient

We also provide some statistical information on our results for a discretization with $\Delta x = 10$: We considered 100 realizations of noise to perturb the given data and solved the corresponding identification problem. The mean value of the respective results is given by

$$(0.018105, 0.018288, 0.018284)^\top,$$

and the covariance matrix of the results reads

$$\begin{pmatrix} 0.030719 & -0.042635 & -0.063932 \\ -0.042635 & 0.059173 & 0.088732 \\ -0.063932 & 0.088732 & 0.133057 \end{pmatrix} \cdot 10^{-5}.$$

The first component of the recovered friction coefficient systematically undershoots the original value while, for the reasons discussed above, the other components were larger than the original values. Moreover, the covariance matrix presents a dependence pattern that corresponds to the effects cause by the coupling in that large values for the first component induce smaller values on the other components and vice versa.

[1] A. Bressan. *Hyperbolic systems of conservation laws*, volume 20 of *Oxford Lecture Series in Mathematics and its Applications*. Oxford University Press, Oxford, 2000. The one-dimensional Cauchy problem.
[2] A. R. Conn, N. I. M. Gould, and P. L. Toint. *Trust-region methods*. MPS/SIAM Series on Optimization. Society for Industrial and Applied Mathematics (SIAM), Philadelphia, PA; Mathematical Programming Society (MPS), Philadelphia, PA, 2000.
[3] P. Domschke. *Adjoint-Based Control of Model and Discretization Errors for Gas Transport in Networked Pipelines*. PhD thesis, TU Darmstadt, 2011.
[4] P. Domschke, B. Hiller, J. Lang, and C. Tischendorf. Modellierung von gasnetzwerken: Eine übersicht. Technical Report 2717, Technische Universität Darmstadt, 2017.
[5] H. Egger, T. Kugler, and N. Strogies. Parameter identification in a semilinear hyperbolic system. *Inverse Problems*, 33(5):055022, 25, 2017.
[6] Y Farjoun and B. Seibold. Solving one dimensional scalar conservation laws by particle management. *Meshfree methods for partial differential equations IV*, 65:95, 2008.
[7] C. Gotzes, H. Heitsch, R. Henrion, and R. Schultz. On the quantification of nomination feasibility in stationary gas networks with random load. *Math. Methods Oper. Res.*, 84(2):427–457, 2016.
[8] M. Gugat, M. Herty, and V. Schleper. Flow control in gas networks: exact controllability to a given demand. *Math. Methods Appl. Sci.*, 34(7):745–757, 2011.
[9] S. Hajian and M. Hintermüller. Total variation diminishing schemes in optimal control of scalar conservation laws. WIAS Preprint No. 2383, 2017.
[10] F. M. Hante. *Hybrid Dynamics Comprising Modes Governed by Partial Differential Equations: Modeling, Analysis and Control for Semilinear Hyperbolic Systems in One Space Dimension*. PhD thesis, University Erlangen-Nuremberg, 2010.
[11] F. M. Hante and G. Leugering. Optimal boundary control of convention-reaction transport systems with binary control functions. In *HSCC*, pages 209–222. Springer, 2009.
[12] M. Herty, J. Mohring, and V. Sachers. A new model for gas flow in pipe networks. *Math. Methods Appl. Sci.*, 33(7):845–855, 2010.
[13] M. Hintermüller and N. Strogies. On the consistency of runge–kutta methods up to order three applied to the optimal control of scalar conservation laws. WIAS Preprint No. 2442, 2017.
[14] T. Koch, B. Hiller, M. E. Pfetsch, and L. Schewe, editors. *Evaluating gas network capacities*, volume 21 of *MOS-SIAM Series on Optimization*. Society for Industrial and Applied Mathematics (SIAM), Philadelphia, PA, 2015.
[15] O. Kolb, J. Lang, and P. Bales. An implicit box scheme for subsonic compressible flow with dissipative source term. *Numer. Algorithms*, 53(2-3):293–307, 2010.
[16] R. J. LeVeque. *Finite volume methods for hyperbolic problems*. Cambridge Texts in Applied Mathematics. Cambridge University Press, Cambridge, 2002.
[17] J. Nocedal and S. J. Wright. *Numerical optimization*. Springer Series in Operations Research and Financial Engineering. Springer, New York, second edition, 2006.
[18] S. Pfaff, S. Ulbrich, and G. Leugering. Optimal control of nonlinear hyperbolic conservation laws with switching. In *Trends in PDE constrained optimization*, volume 165 of *Internat. Ser. Numer. Math.*, pages 109–131. Birkhäuser/Springer, Cham, 2014.
[19] L. Qi and J. Sun. A nonsmooth version of Newton's method. *Math. Program.*, 58(3 (A)):353–367, 1993.
[20] B. L. Rožd̆estvenskiĭand N. N. Janenko. *Systems of quasilinear equations and their applications to gas dynamics*, volume 55 of *Translations of Mathematical Monographs*. American Mathematical Society, Providence, RI, 1983. Translated from the second Russian edition by J. R. Schulenberger.
[21] J. Stolwijk and V. Mehrmann. Error analysis and model adaptivity for flows in gas networks. *Analele Stiintifice Univ. Ovidius Constanta. Seria Matematica*, 2017. Accepted for publication.
[22] D. Sun and L. Qi. On NCP-functions. *Comput. Optim. Appl.*, 13(1-3):201–220, 1999. Computational optimization—a tribute to Olvi Mangasarian, Part II.
[23] S. Ulbrich. *Optimal Control of Nonlinear Hyperbolic Conservation Laws with Source Terms*. habilitation, TUM, 2001.
[24] A. Zlotnik, M. Chertkov, and S. Backhaus. Optimal Control of Transient Flow in Natural Gas Networks. *ArXiv e-prints*, April 2015.